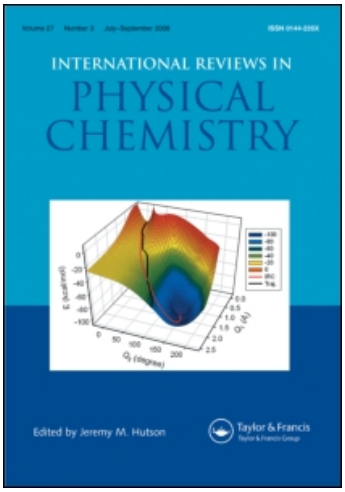

International Reviews in Physical Chemistry
Publication details, including instructions for authors and subscription information:
http://www.informaworld.com/smpp/title~content=t713724383

Synchrotron X-ray diffraction studies of inorganic materials and heterogeneous catalysts

J. M. Newsam[a]; K. S. Liang[a]
[a] Exxon Research and Engineering Company, Annandale, New Jersey, USA

To cite this Article Newsam, J. M. and Liang, K. S.(1989) 'Synchrotron X-ray diffraction studies of inorganic materials and heterogeneous catalysts', International Reviews in Physical Chemistry, 8: 4, 289 — 338
To link to this Article: DOI: 10.1080/01442358909353232
URL: http://dx.doi.org/10.1080/01442358909353232

INTERNATIONAL REVIEWS IN PHYSICAL CHEMISTRY, 1989, VOL. 8, NO. 4, 289–338

Synchrotron X-ray diffraction studies of inorganic materials and heterogeneous catalysts

by J. M. NEWSAM and K. S. LIANG

Exxon Research and Engineering Company, Route 22 East, Annandale, New Jersey 08801, U.S.A.

The special features of synchrotron X-radiation and the types of instrumentation required for a range of synchrotron X-ray diffraction experiments are outlined. A diverse range of applications to inorganic and heterogeneous catalyst systems are discussed. Grazing incidence X-ray diffraction experiments have revealed a number of surface structures and followed surface phase transformations; similar studies of boundary and interfacial structures are cited. Experiments on catalytic metals dispersed on supports have exploited anomalous scattering effects. High-resolution powder diffraction has assisted phase identifications, provided quantitative data on peak broadening (such as arise from particle size effects or stacking disorder), enabled studies of subtle superstructures and a growing number of *ab initio* structure solutions, and permitted Rietveld refinements of a range of inorganic materials. The potential for performing measurements on individual crystallites in the micrometre size regime has been demonstrated; a small number of successful single-crystal structure refinements have been described. Single-crystal Laue methods have been also applied successfully to structure refinements and solutions; this configuration potentially permits data sufficient for structure definition to be recorded on a nano-microsecond time scale. A range of studies that are time-resolved (currently on somewhat longer scales), and various studies under non-ambient conditions (such as at high or low temperatures, at extreme pressures, or under applied magnetic and electric fields) have also been described. These various applications of synchrotron X-ray diffraction techniques to inorganic and heterogeneous catalyst systems both illustrate already substantial contributions to our understanding, and promise still greater advances from future applications.

1. Introduction

Diffraction experiments have been the source of much of our understanding of the structures of solids, and of our appreciation of those properties which are related directly to structure. Following the discovery of X-rays by Röntgen in 1895, early descriptions of diffraction theory by M. von Laue in 1912, and the first crystal structure determinations by W. H. and W. L. Bragg in 1912, progress in the application of diffraction methods (using X-rays, electrons, neutrons and gamma-rays) has been spectacular. Each new decade has witnessed major advances. Over the past 15 years, certainly one of the most prominent advances has been the advent of the synchrotron X-ray source for diffraction experiments. The particular qualities of synchrotron X-radiation that are introduced below are such as to allow a new generation of diffraction experiments. Although many synchrotron X-ray diffraction techniques are still at relatively early stages of development, such experiments have already contributed significantly to our understanding of solid state inorganic chemistry and catalyst science and it is an appropriate time to overview both the contribution that such techniques have already made and the areas of particular promise currently under development.

0144–235X/89 $3·00

Industrial catalysis has developed largely as an empirical art. Chance has played a significant role in initial discoveries of new catalysts or new processes, and Edisonian 'trial-and-error' adjustments have allowed process and catalyst improvements. Although the potential for major process advances that a deeper scientific understanding promises has long been recognized, the complexities of most real catalyst systems have proven too demanding for complete study by available characterization and theoretical tools. Commercial catalysts are typically multiphase composites, with different constituents playing both distinct and interacting roles. Catalytically active centres are usually dilute, and confined to surface or interfacial regions. Process conditions are often difficult to reproduce, involving elevated temperatures and/or pressures, and reactive environments. As we discuss further below, the opportunities offered by synchrotron X-ray diffraction extend to these more taxing regimes of low concentration, multiple phases and non-ambient conditions. Measurements using synchrotron radiation of the extended X-ray absorption fine structure (EXAFS) of metals in, for example, reforming catalysts already have a proven track record of contributions to heterogeneous catalyst science. There is every reason to anticipate that the more detailed and more precise structural data provided by diffraction experiments will have a still larger impact.

2. The synchrotron X-ray source

A synchrotron comprises an approximately circular vacuum chamber around which are placed bending magnets, quadrupole magnets for focusing and radio-frequency (r.f.) cavities that accelerate groups of electrons from a low injection energy to a peak energy some 10–100 times higher. A storage ring (the machine configuration actually used for all current dedicated synchrotron radiation sources) is similar, but is designed to maintain bunches of electrons in orbit at constant energy (after an initial injection cycle; groups of electrons are generally injected at substantially lower energy (0·75 GeV at the National Synchrotron Light Source (NSLS) at Brookhaven National Laboratory) and require initial acceleration to the operating energy (2·5 GeV for the X-ray ring at NSLS). As the bunches of high-energy electrons follow circular orbits through the bending magnet sections they emit synchrotron radiation (SR). The emission of synchrotron radiation by electrons travelling in circular orbits at relativistic velocities (Koch 1983, Kunz 1979, Marr 1987, Moncton and Brown 1990, Sokolov and Ternov 1968, Winick 1987, Winick and Doniach 1980) was considered theoretically as early as 1898. Experiments in the late 1940s on the General Electric 70 MeV synchrotron confirmed many of the predicted properties of this radiation. These remarkable properties, which are discussed in more detail subsequently, begin to develop only when the speed of the circulating electrons approaches the speed of light. At lower velocities, the radiation emitted as the electrons undergo centrifugal acceleration is emitted almost isotropically. As their speed approaches that of light, the radiation becomes focused tightly into a cone in the forward direction (figure 1) with a divergence angle θ_v given by

$$\theta_v \sim \gamma^{-1}; \quad \gamma = \frac{E}{m_o c^2} = 1{\cdot}957 \times 10^3 \, E(\text{GeV}) \tag{1}$$

The divergence of radiation emitted from a synchrotron X-ray source is thus extremely small, of the order of 0·2 mrad (compared to the isotropic emission from a conventional target source). This low divergence has a number of advantages. It corresponds to a fine degree of resolution on the incident beam direction, and hence to easily obtainable high

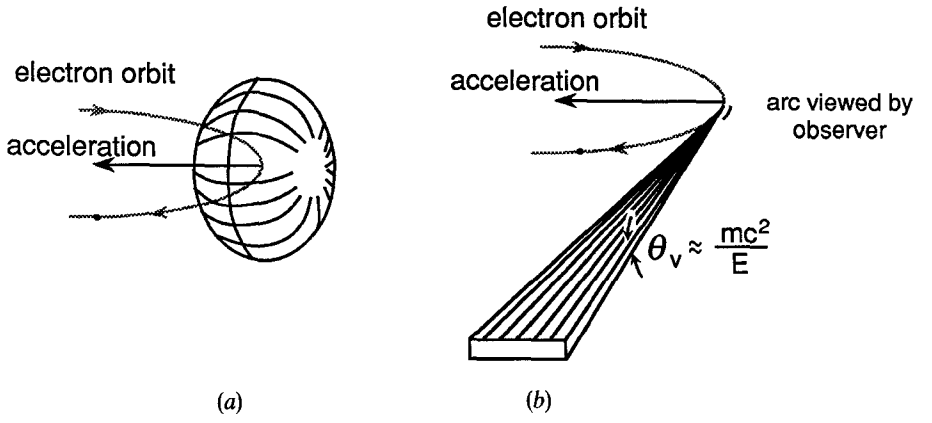

Figure 1. The radiation emitted by an electron following a circular path is emitted near isotropically at low energies but, at relativistic velocities, the radiation is focused tightly in the forward direction. (*a*) $v/c \ll 1$, (*b*) $v/c \approx 1$.

resolution conditions. Attainment of similar definition in-house is also possible, but at the expense of rejecting much of the radiation from an already lower-emittance source. With low source divergence, optimal use of X-ray optics technology can be made, for example in the use of mirrors that redirect and focus the beam by total external reflection at glancing angles, and in the use of high-quality single crystals (e.g. Si and Ge) as monochromators. It is therefore more appropriate to talk in terms of the source brightness, in units of photons eV^{-1} $mrad^{-1}$ s^{-1}, which proves to be the key parameter in determining the feasibility of a number of types of diffraction experiment. In terms of brightness, a typical SR source is more intense than a fine focus tube at a characteristic Kα emission line (such as Cu Kα) by many orders of magnitude.

The spectrum of radiation emitted by a relativistic electron describing a circular orbit is continuous down to a critical wavelength, λ_c (or up to a critical energy, E_c (keV) = 12399/λ_c(Å), see figure 2) which is determined by the energy of the electrons and the tortuosity of the path that they follow (expressed as the radius of orbit curvature, ρ)

$$\lambda_c = \frac{4\pi\rho}{3\gamma^3}. \tag{2}$$

A conventional source of X-rays, such as a fine-focus tube or rotating anode source, emits *Bremsstrahlung* radiation which is continuous, but relatively low-level up to a high-energy cut-off determined by the accelerating voltage (typically 30–50 kV). Superposed on the continuous spectrum are the substantially more intense characteristic emission lines of the element(s) present in the target (usually Cu or Mo). For most types of quantitative diffraction experiment, only the characteristic Kα or Kβ lines are of sufficient intensity to be usable, so that alteration of wavelength requires a change of target material. The broad spectral distribution from the synchrotron source is thus a considerable benefit to the several classes of diffraction experiment for which it is desirable to choose a specific wavelength. Further, the continuous character of the synchrotron source allows huge enhancements in performance for those experiments such as single-crystal Laue diffraction or energy-dispersive powder X-ray diffraction (see below) which can use a broad bite of the incident brightness against wavelength spectrum.

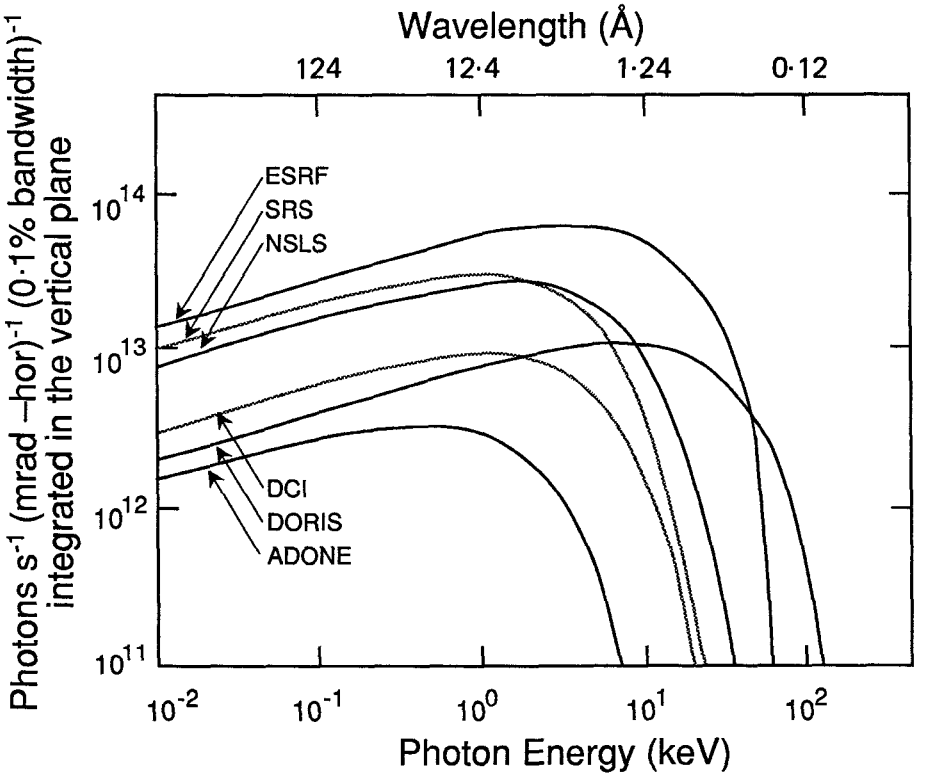

Figure 2. The spectral distribution of emitted synchrotron radiation depends on the storage ring current and energy, and the structure of the magnet section within which the electron paths are undergoing radial acceleration. The critical energy, the energy above which the emitted photon flux diminishes rapidly, also depends on the ring energy and magnet section structure. The spectral distribution is shown for bending magnets at six different storage rings (see table 3) (after Koch (1983)).

In the exact orbital plane, the synchrotron radiation is 100% linearly polarized (with the electromagnetic field vector parallel to the electron radial acceleration direction). Deviations from perfect planarity of the orbit contribute some perpendicular polarization component to the usable photon flux. These deviations are small, and in a typical diffraction experiment that exploits a relatively small (vertical) window of the radiation, the effective horizontal polarization exceeds 90%. Although some experiments, such as those of circular dichroism (Templeton and Templeton 1985, 1989) or magnetic scattering (Gibbs *et al.* 1988), can exploit the high level of polarization, for most diffraction experiments it represents a constraint which influences the design and orientation of measuring equipment.

To maintain the trajectory of the electrons in the ring at constant energy, energy must be supplied continually in the form of r.f. pulses. The electrons in the ring are grouped in small bunches that pass sequentially around the ring through the r.f. sections (figure 3). The bunch structure and filling is a particular ring characteristic, but at the NSLS (operating energy of 2·5 GeV), the time width of a bunch at a given point in the ring is of the order of 1·7 ns (10^{-9} s) with a bunch separation of about 19 ns. The time taken for a single bunch to circuit the ring is about 570 ns (table 1). Experiments can be designed to exploit these time scales (Mills 1984). For example, the ~20 ns bunch

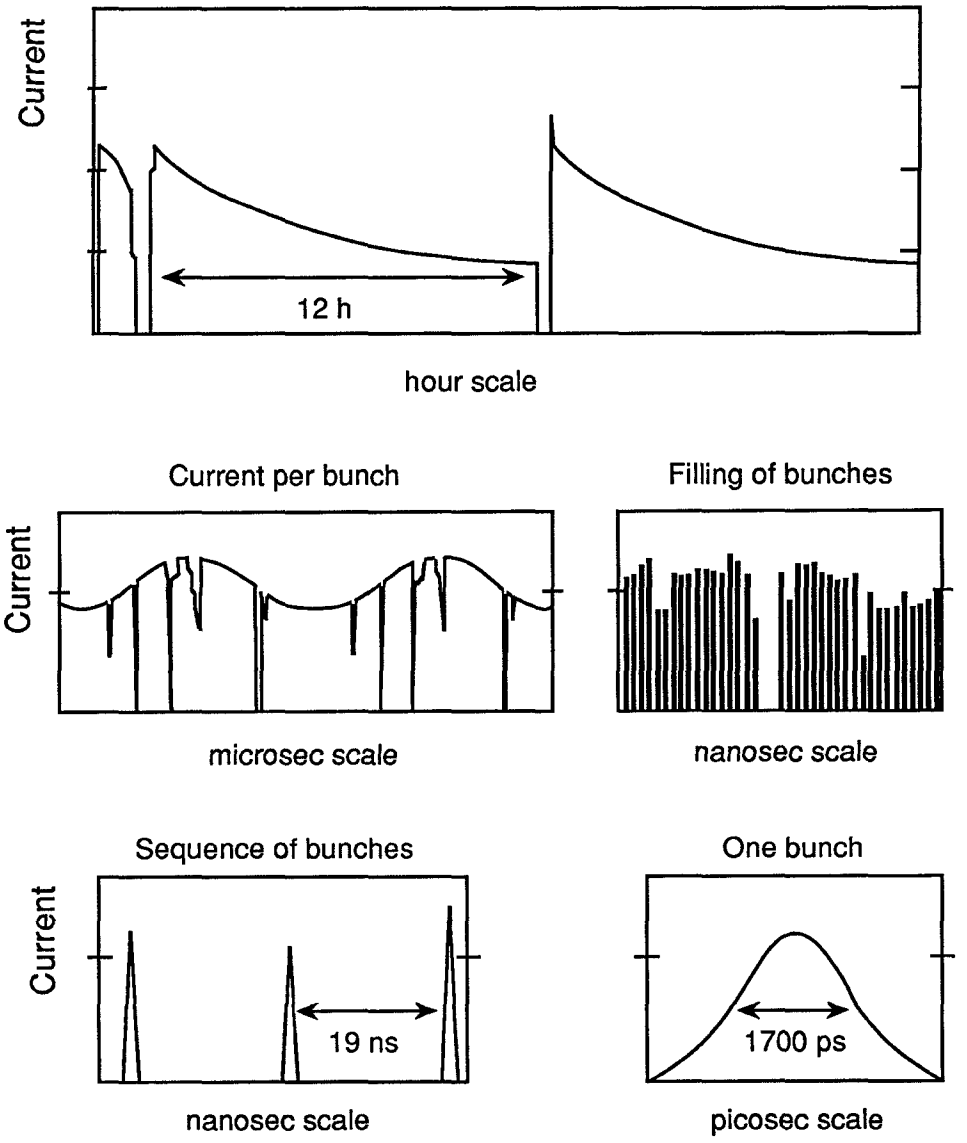

Figure 3. The ring current is carried in a discrete number of electron bunches so that the radiation received by a particular experiment is pulsed on a ~20 ns time-scale. There is some cross-talk between bunches. A much longer time-scale is associated with the global beam dump–inject–ramp–exponential current decay cycle (after Stuhrmann (1988)).

Table 1. Characteristics of U.S.A. storage ring facilities.

	SSRL	CHESS	NSLS	6 GeV
λ_c	2·64	1·43	2·48	0·78
Orbit period (ns)	760	2560	568	2670
Number of bunches	1 (4)	1 (7)	30	1 (10)
Bunch duration (ps)	300	160	1700	100
Interpulse period (ns)	760 (190)	2560 (366)	18·9	2670 (267)

separation could, with suitable gating, be used to study phenomena that occur with characteristic times in this range, or the application of an external impulse (such as a laser pulse) could be synchronized so that the time evolution of the system is followed (such measurements of course require a high degree of sophistication in the measuring equipment). Many motional and reactive processes occur over time scales longer than several nanoseconds, and the potential for tracking such structural or chemical changes remains largely to be explored. The use of synchrotron X-ray diffraction techniques for performing kinetic studies on catalysts is one area that is likely to blossom over the next decade.

A much longer time period (several hours) is associated with the filling and decay of the electron current in the storage ring (figure 3). As introduced earlier, all present facilities use an injection system that delivers electrons into the ring at substantially less than the operating energy. This filling process takes place iteratively over many minutes. Following filling to the target current level, the ring is configured to ramp the electron energy from the injection energy to operating energy. The orbit is stabilized and beam is then made available to experiments. At this point the beam is at its most intense, although because of inevitable losses in the ring, the current decays exponentially with time, with a characteristic half-time of a few hours (figure 3). Unforeseen mechanical, electrical, vacuum or user problems may cause premature beam dumps. As discussed further below, diffraction experiments must be designed to cope with these temporal changes in the state of the source. Problems with orbit control, stability and reproducibility from fill to fill, combined with mechanical problems associated partly with the varying heat loads deposited on the X-ray optics were key factors limiting the early development of synchrotron X-ray diffraction techniques. The situation at today's dedicated facilities is much improved.

To summarize, the synchrotron source provides extremely intense X-ray beams which have low intrinsic divergence, are continuous over a broad range of wavelengths, and have a well defined time structure. Each of these properties provides new opportunities for diffraction experiments (table 2) and several of these opportunities have been exploited in studies of systems of interest in catalysis (De Angelis *et al.* 1987, Nomura 1988).

Table 2. Opportunities for diffraction experiments to exploit the special features of synchrotron X-radiation.

High source brightness (intensity + natural collimation)	Surface crystallography High-resolution diffraction (spatial/scattering vector–single crystal/powder) Subtle superstructures Microcrystal diffraction
Broad spectral range	Single-crystal Laue diffraction Energy-dispersive X-ray scattering Anomalous scattering
Pulsed time structure	Stroboscopic diffraction ^{57}Fe Mössbauer diffraction
High polarization	X-ray dichroism Magnetic scattering

The present status of the world's major synchrotron X-radiation facilities is listed in table 3. Capabilities represented in the experimentation at each of these facilities vary somewhat, although most have beam lines suitable for performing surface X-ray diffraction, wavelength dispersive scattering modes or studies exploiting anomalous scattering, and single crystal and powder diffraction. High-pressure work is generally represented and the degree to which catalyst studies are pursued varies considerably from facility to facility. Absorption measurements such as EXAFS and near-edge X-ray absorption fine structure (NEXAFS) (Bart 1986) have been made at all major centres. Although not discussed here, EXAFS measurements (Teo 1986) have revealed local structural information for a wide range of catalyst systems (Bart and Vlaic 1987, Greaves 1988, Joyner and Meehan 1983, Kochubei and Zamaraev 1985) such as those of interest in reforming (Koningsberger *et al.* 1986, Koningsberger and Sayers 1985, Meitzner *et al.* 1988, 1987, Sinfelt 1983, Sinfelt *et al.* 1978, 1984, Via *et al.* 1983), hydrodesulphurization (Boudart *et al.* 1983, Clausen *et al.* 1986), methanol (Sankar *et al.* 1986) and ammonia synthesis (Clausen *et al.* 1989), methanol carbonylation (Denley *et al.* 1984), V_2O_5–TiO_2 oxidation catalysts (Kozlowski *et al.* 1983a, b, c) and metal particles within zeolites (Moller *et al.* 1989b, Moraweck *et al.* 1986, Tzou *et al.* 1986, Yokoyama *et al.* 1986). In many cases measurements have been made at close to process conditions (Boudart *et al.* 1985). These data have contributed substantially to our understanding of catalyst function.

Table 3. Storage ring synchrotron radiation sources.

Location	Ring (laboratory)	Electron energy (GeV)	Status
Brazil			
Campinas	LNLS	2·0	Dedicated†
Peoples Republic of China			
Beijing	BEPC (IHEP)	2·2–2·8	Partly dedicated
Hefei	HESYRL (USTC)	0·8	Dedicated†
England			
Daresbury	SRS (Daresbury)	2·0	Dedicated
France			
Orsay	ACO (LURE)	0·54	Dedicated
	DCI (LURE)	1·8	Dedicated
	Super ACO (LURE)	0·8	Dedicated
Grenoble	ESRF	6·0	Dedicated†
Germany (Federal Republic)			
Bonn	ELSA	3·5	Partly dedicated
Dortmund	DELTA	1·5	Design†
Hamburg	DORIS II (HASYLAB)	3·5–5·5	Partly dedicated
West Berlin	BESSY	0·8	Dedicated
	BESSY II	1·5–2·0	Design/dedicated†
India			
Indore	INDUS–I (CAT)	0·45	Design/dedicated†
	INDUS–II (CAT)	1·5–2·0	Design/dedicated†
Korea			
Pohang	Pohang Light Source	2·0	Partly dedicated†

Table 3 (*continued*)

Location	Ring (laboratory)	Electron energy (GeV)	Status
Italy			
Frascati	ADONE (LNF)	1·5	Partly dedicated
Trieste	Sincrotrone Trieste	1·5–2·0	Dedicated†
Japan			
Okasaki	UVSOR (IMS)	0·6	Dedicated
Kansai		6·0	Design/dedicated†
Tokyo	SOR (ISSP)	0·4	Dedicated
Tsukuba	TERAS (ETL)	0·6	Dedicated
Tsukuba	Photon Factory (KEK)	2·5	Dedicated
	Accumulator (KEK)	6·0–8·0	Partly dedicated
	TRISTAN (KEK)	25–30	Parasitic†
Sweden			
Lund	Max (LTH)	0·55	Dedicated
Taiwan (Republic of China)			
Hsin Chu	TLS (SRRC)	1·3	Dedicated†
U.S.A.			
Argonne, IL	APS (ANL)	7·0	Dedicated†
Berkeley, CA	ALS (LBL)	1·5	Dedicated†
Gaithersburg, MD	SURF II (NBS)	0·28	Dedicated
Ithaca, NY	CESR (CHESS)	5·5–8·0	Partly dedicated
Stanford, CA	SPEAR (SSRL)	3·0–3·5	Partly dedicated
	PEP (SSRL)	5·0–15·0	Partly dedicated
Stoughton, WI	Aladdin (SRC)	0·8–1·0	Dedicated
Upton, NY	NSLS I (BNL)	0·75	Dedicated
	NSLS II (BNL)	2·5	Dedicated
Baton Rouge, LA	CAMD (LSU)	1·0	Dedicated†
U.S.S.R.			
Karkhov	N–100 (KPI)	0·10	Dedicated
Moscow	Siberia I (Kurchatov)	0·45	Dedicated
	Siberia II (Kurchatov)	2·5	Dedicated†
Novosibirsk	VEPP–2M (INP)	0·7	Partly dedicated
	VEPP–3 (INP)	2·2	Partly dedicated
	VEPP–4 (INP)	5·0–7·0	Partly dedicated

† In planning, construction or commissioning.

3. Synchrotron X-ray instrumentation and operation

The layout of a typical beam line which can be configured for absorption or scattering experiments (Exxon beamline X10A at the National Synchrotron Light Source, Brookhaven National Lab.) is illustrated in figures 4 and 5. A swath 3·7 mrad wide of radiation emitted from the bending magnet is intercepted by a bent cylindrical platinum-coated quartz mirror, which focuses the radiation in both horizontal (cylindrical cut) and vertical (bend) senses at the sample position. The radiation incident on the mirror is trimmed by pre-mirror slits, and the attitude and degree of bend in the mirror are adjustable so as to vary the position and quality of the focus. The mirror can be lowered out of the beam, and the components downstream restored to a level orientation (the take-off angle from the mirror is some 4·8 mrad in focused mode)

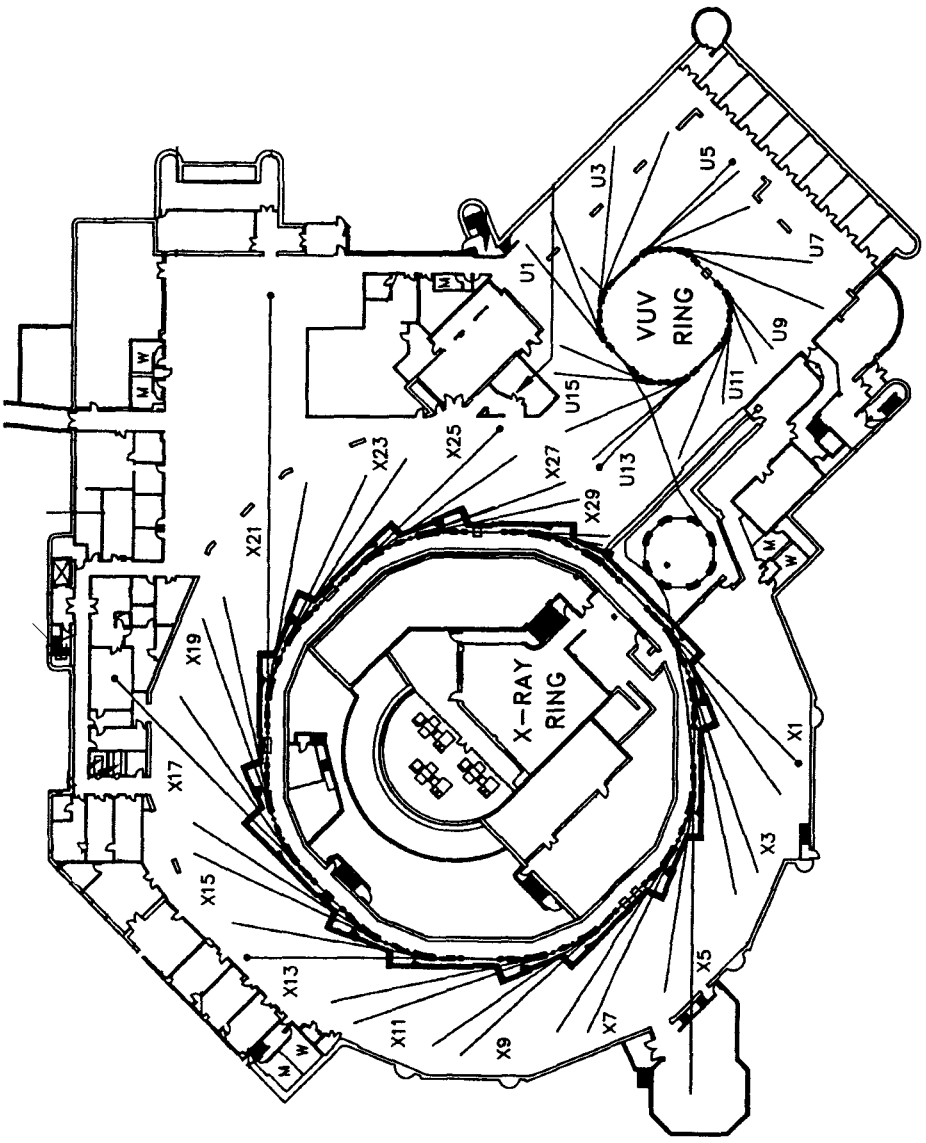

Figure 4. Layout of the X-ray and vacuum ultraviolet (VUV) storage rings at the National Synchrotron Light Source (NSLS) at Brookhaven National Laboratory (after Gmür *et al.* (1989)).

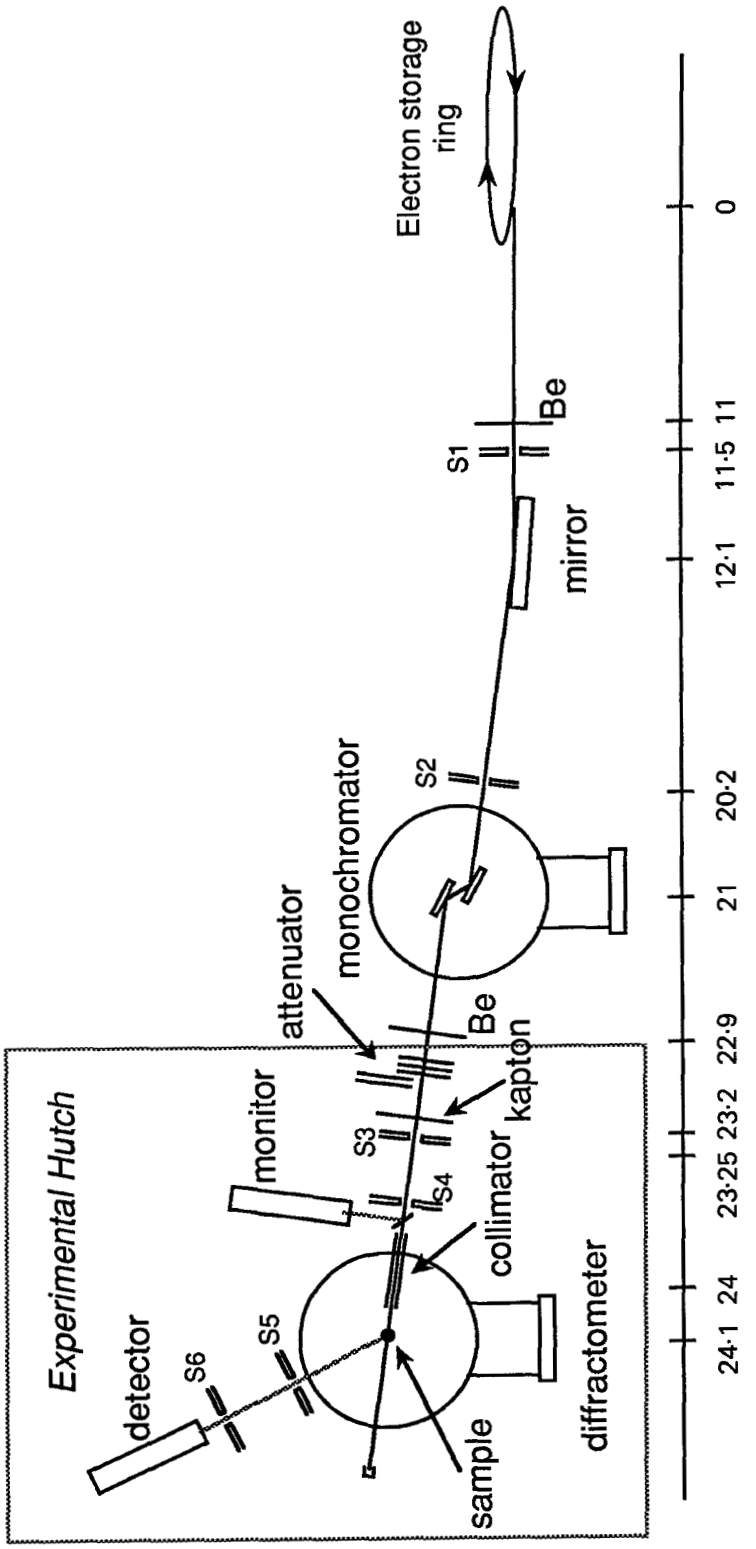

Figure 5. Layout of a typical synchrotron hard X-ray beam line (Exxon beam line X10A at NSLS) used for diffraction and absorption experiments on inorganic and catalyst materials.

so as to permit experiments with an unfocused beam if required. The mirror and pre-mirror slits are water-cooled, although the temperature of the mirror surface changes by several degrees during the fill–beam available–beam dump cycle.

The monochromator is typically a parallel pair of flat, perfect Si or Ge crystals, although a wide range of monochromator designs have been considered and several types are actually implemented at existing facilities. By using a pair of mechanically-coupled parallel monochromator crystals, the wavelength selected for the experiment can be continuously varied without changing the direction of the beam impinging on the sample. Rapid selection of a desired wavelength, and energy dispersive scans, such as EXAFS measurements are, therefore, possible.

Monochromator crystals can be fabricated so as to yield near-perfect scattering characteristics, with an energy spread in the diffracted beam determined by the rocking-curve width, ω, which, for a perfect crystal, is given by the Darwin formula

$$\omega = \frac{2}{\sin 2\theta_B} \frac{(e^2/mc^2)\lambda^2}{\pi V} C|F_h| \exp(-M), \tag{3}$$

where θ_B is the Bragg angle, V the unit cell volume, $|F_h|$ the modulus of the structure factor, $\exp(-M)$ the temperature factor and C the polarization factor. The band pass is thus narrower for lower atomic number materials (for which $|F_h|$ is smaller—physically this can be rationalized in terms of the larger number of diffracting planes sampled in a lower-scattering material). The Si (111) reflection, for example, gives a factor of about three smaller energy spread than Ge (111) (table 4). The band pass is also narrower for higher order reflections (figure 6, larger $\sin 2\theta_B$ and smaller $|F_h|$ (and $\exp(-M)$), although with correspondingly lower integrated reflectivities). The monochromator band pass is one of the factors determining the resolution in a diffraction experiment, and for typical monochromator crystals such as Si (111) or Ge (111) is of the order of $\Delta\lambda/\lambda = \Delta d/d = \Delta E/E = \Delta\theta \cot\theta = 1\text{–}3 \times 10^{-4}$ (table 4).

A single crystal in the (111) orientation at a given take-off angle diffracts both the primary wavelength from the (hkl) planes and the higher order harmonics ($\lambda/2$, $\lambda/3$, etc.) from the higher order planes, ($(2h\,2k\,2l)$, $(3h\,3k\,3l)$, etc.). This higher order contamination can cause problems or ambiguities in diffraction experiments. The shorter wavelength components may be eliminated by using a mirror (which has a low-wavelength cut-off for total external reflection), energy discrimination in the detector (and monitor), or by slight misalignment of the second monochromator crystal when a parallel pair is used (the degree of misalignment is chosen so that the second crystal captures little of the narrower band pass of the higher order component(s) from the first crystal, figure 6).

Table 4. Characteristics of typical monochromator crystals.

Material	Lattice constant	Planes	d spacing	$\Delta E/E$
Ge	5·65754	111	3·2664	$3{\cdot}2 \times 10^{-4}$
		220	2·0002	$1{\cdot}5 \times 10^{-4}$
Si	5·43102	111	3·1356	$1{\cdot}2 \times 10^{-4}$
		220	1·9202	$5{\cdot}6 \times 10^{-5}$
LiF	4·0270	200	2·0135	$\sim 1 \times 10^{-3}$
C(HOPG)	$a = 2{\cdot}461, c = 6{\cdot}708$	002	3·354	$3{\cdot}8 \times 10^{-2}$

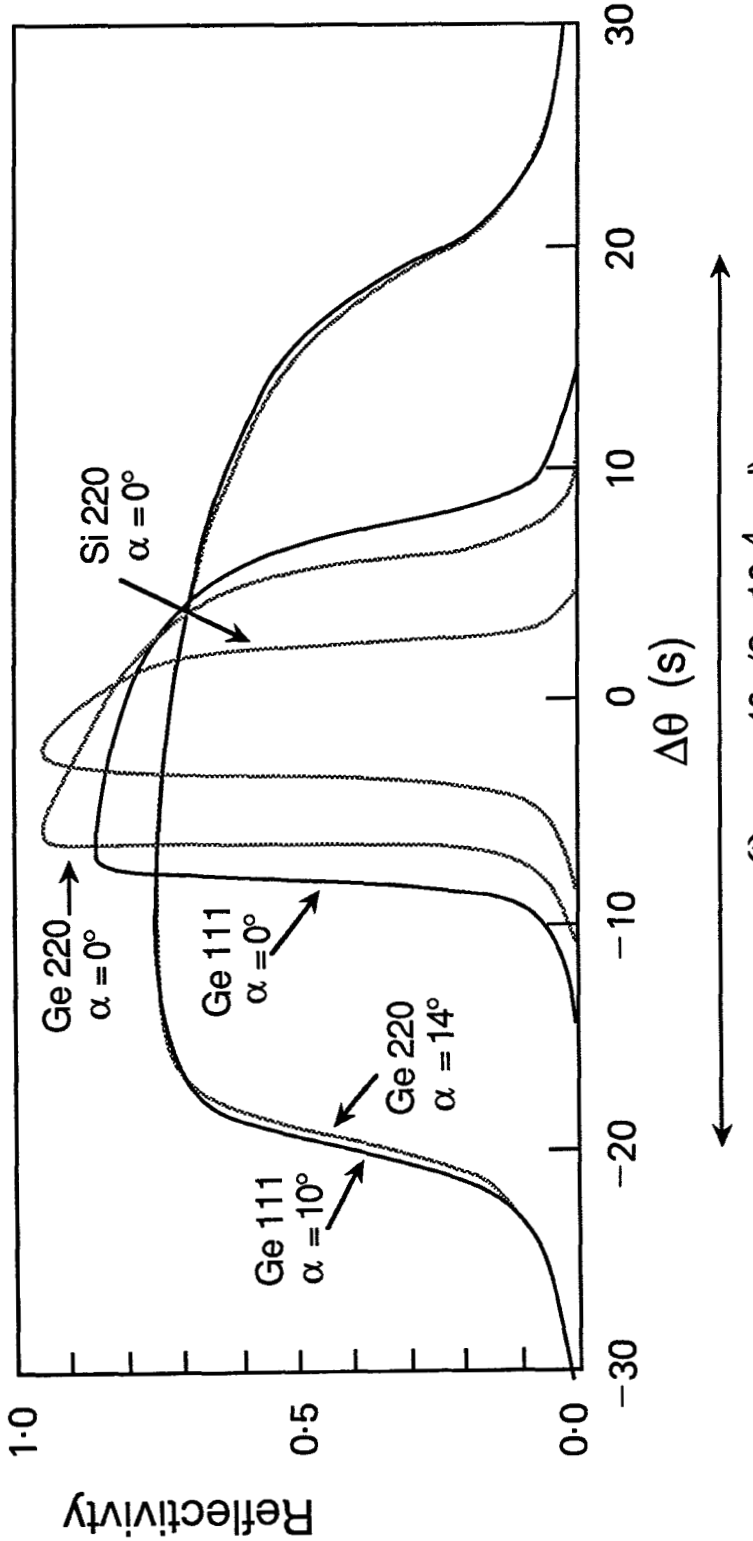

Figure 6. Reflectivity curves for various perfect crystal monochromator configurations. The band pass of the monochromator depends on the atomic number, and the order of the diffracting planes. Data are shown for differing angles of crystal cut, α, with respect to the Bragg planes (after Helliwell (1984)).

Although less convenient for wavelength adjustment, single monochromator crystals might also be used, in a configuration similar to that shown in figure 5 (diffracting vertically) or, as has been implemented on X10B at NSLS (Hewitt *et al.* 1989), diffracting horizontally, close to the plane of the synchrotron ring (figure 7). This line has a cylindrical Pt-coated quartz mirror at 13 m, and the single monochromator crystal at 14–16 m. This configuration has the advantage at X10 of creating more space for experiments, although it entails a slight reduction in delivered X-ray intensity owing to polarization effects. Additionally, a combination of Fankuchen asymmetry in the crystal cut and a slight degree of bend can optimize beam collimation and focusing at the sample position (Fankuchen 1937, Greenhough *et al.* 1983, Hewitt *et al.* 1989). Even with this mechanical bending of the crystal, it proves possible to approximate the band pass permitted by an unstrained perfect crystal.

For most hard X-ray experiments, the beamline components are isolated from the ring vacuum (typically $< 10^{-9}$ Torr) by switchable valves and beryllium windows. For soft X-ray experiments (X-ray energies $< \sim 0{\cdot}8$ keV), such as EXAFS measurements on the lighter elements, or photoemission studies, the low-energy cut-off determined by absorption by the Be windows is undesirable, and direct connection of the experiment to the ring-vacuum can be made, using suitable differential pumping and with ring vacuum protected by fast-acting valves in the event of experiment mishap.

During the phase of injecting and accelerating electrons in the ring, the beam is unavailable to experiments. Immediately completing acceleration, the source brightness is at its highest, although beamline components that have cooled down during the beam dump and fill process require some period to readjust to the new thermal loads. The remainder of the fill, which usually lasts for some 1–23 h depending on the facility, is then providing usable photons for the experiment. The cyclical nature of today's SR sources (figure 3) imposes significant constraints on the design of beam line components such as in management of the thermal loads deposited by the high-intensity photon beam, particularly when components are operating *in vacuo*. The possibility of future facilities operating in 'top-up' mode, in which decay of the stored electrons in the ring is compensated on an ongoing basis by re-injection at ring energy, is clearly attractive. Such a mode would enable operation of the facility and all beam line components essentially in a steady state mode, easing problems associated with maintaining a rigorously stable beam.

The beam, following entry into the experimental hutch, becomes the province of the diffractionist (most facilities control access to the areas to which beam is admitted by a

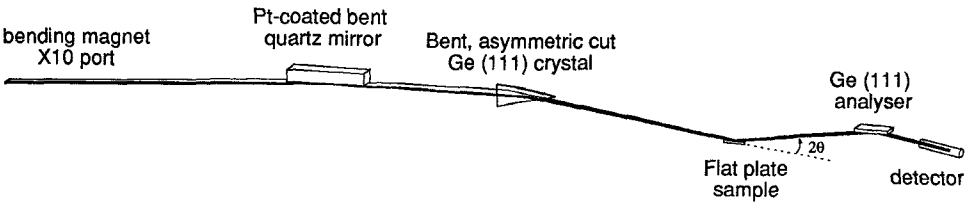

Figure 7. Schematic representation of the Exxon beamline X10B at the National Synchrotron Light Source, Brookhaven. Radiation from a bending magnet port is reflected by a Pt-coated quartz mirror and monochromated by diffraction in the (near-) horizontal plane from a triangular, asymmetric cut Ge (111) crystal. The Frankuchen asymmetric cut provides collimation; the bending permits horizontal focusing of a narrow wavelength band at the sample position. For powder diffraction work, the diffracted beam resolution may be defined by slits or, as shown here, by an analyser crystal.

keyed interlock system that guards against access while the beam is on, figure 5). Within the hutch three components are generally required for diffraction experiments; an incident flight path for collimating and monitoring the incident beam, as well as minimizing stray scattering which might contribute to background; a diffractometer or sample support for accepting and, if necessary, aligning the sample; and a detection system for monitoring the scattered signal, typically as a function of scattering angle (figure 5). The intensity of the synchrotron X-ray beam is such that scattering by air, even over relatively short distances, can give rise to significant and troublesome background. At longer X-ray wavelengths, attenuation of the beam due to air scattering can also be significant. The incident beam definition system is, therefore, typically an evacuated flight path that includes both defining slits or collimators and an incident beam intensity monitor. The temporal fluctuations in the source (both in intensity and sometimes in position/direction) dictate that the intensity incident on the sample be carefully and accurately monitored. A typical monitor comprises a thin sheet of Kapton or beryllium inclined at about 45° to the beam direction that scatters a small portion of the radiation towards a vertical scintillation counter. This arrangement is adequate for, for example, powder diffraction experiments, although it has a wide catchment area and provides little indication of small changes in beam direction. It can therefore prove unreliable in diffraction experiments on very small samples (see below).

For most of the diffraction experiments mentioned further below, the sample is mounted on a two-circle (2θ–ω), four-circle (2θ–ω–χ–ϕ), or six-circle (2θ–ω–χ–ϕ; 2θ–ω rotations for an analyser crystal on the diffracted beam) diffractometer, depending on the degree to which sample orientation must be specified, and on the character of the detection system. Of increasing importance, particularly in studies of catalyst systems, is an ability to control the environment of the sample during the diffraction measurements. Although EXAFS experiments under relatively rigorous near-process conditions are often made, diffraction experiments on systems of interest in catalysis have, in the main, been performed under ambient conditions.

The detection system varies from conventional photographic film (for single-crystal Laue diffraction experiments), a single scintillation detector (with the solid scattering angle recorded determined by slits or by an analyser crystal, see below), a linear position-sensitive detector (generally with the long axis spanning a range of scattering angles), or an area detector. As will become plain below, area detectors offer a number of potential advantages, and several configurations are being optimized for synchrotron X-ray diffraction applications (see for example Amemiya *et al.* (1988), Milch *et al.* (1982) and Prieske *et al.* (1983)).

The continuous character of the synchrotron X-ray source permits measurements in energy-dispersive mode. Such a scan can be accomplished (using the arrangement illustrated in figure 5) at a fixed Bragg angle by varying the incident wavelength. Alternatively, a white incident beam may be used, with a (fixed) energy-dispersive detector. The latter mode permits extended regions of the complete diffraction profile to be accumulated in a very short time frame. Further, the use of fixed incident and diffracted beam directions facilitates the use of sample environment control apparatus, such as a high-pressure cell. Energy dispersive diffraction studies of systems under extreme pressure are being conducted at most of the major synchrotron facilities (Skelton 1984). The resolution afforded by today's energy dispersive detectors is of the order of 150–250 eV (compared to the Si (111) bandpass of some 2 eV at 8 keV, table 4), permitting powder diffraction profiles to be obtained at moderate resolution (Bordas *et al.* 1977), with peak shapes that have been found, conveniently, to be Gaussian

(Buras 1980, Buras *et al.* 1979). Corrections need to be applied to the measured pattern for the distribution of incident intensity with wavelength, and for wavelength dependent scattering and absorption processes within the sample. Some relatively simple systems have been studied quantitatively (Buras *et al.* 1979).

Most of the major synchrotron X-ray facilities (table 3) have programmes that enable ready access to the general scientific community. The facilities each have an in-house staff expert in the properties of synchrotron radiation, and in the characteristics of the various beamline components. The interested user can, therefore, focus his attention on the details of his or her specific experiment(s).

Various generic classes of experiments which exploit the different features of synchrotron radiation are listed in table 2. The subsequent discussion is divided logically by nature of experiment, rather than by the material on which experiments have been based. However, although much of the early work on synchrotron X-ray diffraction mentioned here has focused on developing and exploring techniques, various classes of materials of current topical interest have been examined. We shall for example, mention explicitly a range of experiments on mixed metal oxides, microporous materials such as zeolites, metal surfaces and metals dispersed on oxide supports.

4. Atomic level surface structure

The mosaic character and nature of imperfections in extended crystal surfaces can be examined by topography (a spatially-resolved diffraction technique) for which synchrotron radiation offers advantages (Graeff 1985, Hart 1975, Kuriyama *et al.* 1982, Tuomi *et al.* 1974). A number of interesting studies have been reported, including studies of twinning (Docherty *et al.* 1988), polytypism (Fisher and Barnes 1984), GaAs (Kuriyama *et al.* 1988) and organic crystals (Roberts *et al.* 1983), although as yet none are of direct relevance to catalysis.

The prime difficulty in studies of atomic level surface structure (Van Hove and Tong 1985) is that of concentration. Even for a reasonably sized surface of the order of a few square millimetres, the number of atoms comprising a surface structure or an adsorbed layer is quite small (10^{13}–10^{15}). Conventional studies of structure have, therefore, relied heavily on low-energy electron diffraction (LEED) (Van Hove and Tong 1979), where the low concentration can be offset by high scattering cross-sections, albeit with the difficulty then of interpreting diffracted intensities in a quantitative fashion because of multiple-scattering effects. The brightness available at the synchrotron X-ray source has provided new opportunities for surface science, both surface diffraction and other areas such as photoemission from, or X-ray absorption by, species on surfaces.

A key technical development in surface X-ray diffraction was to employ grazing incidence geometry (Marra *et al.* 1979), in which the incident and diffracted beams lie close to coplanar with the surface (figure 8), rather than the conventional configuration in which the scattering vector (the bisector of incident and diffracted beams) is perpendicular to the surface. Practically, the incidence angle of the X-rays is maintained at close to the critical angle for total external reflection. In so doing, the evanescent X-ray wave is limited in its penetration into the bulk to within a shallow skin depth. This both enhances the effective scattering from the surface and, equally importantly, reduces the (background) bulk scattering. Initial experiments on a reconstructed Ge (100) surface by Eisenberger and Marra (1981) demonstrated that, in this experimental configuration, monolayer surface sensitivity was indeed attainable. Over the last decade many other groups have further developed and explored the utility

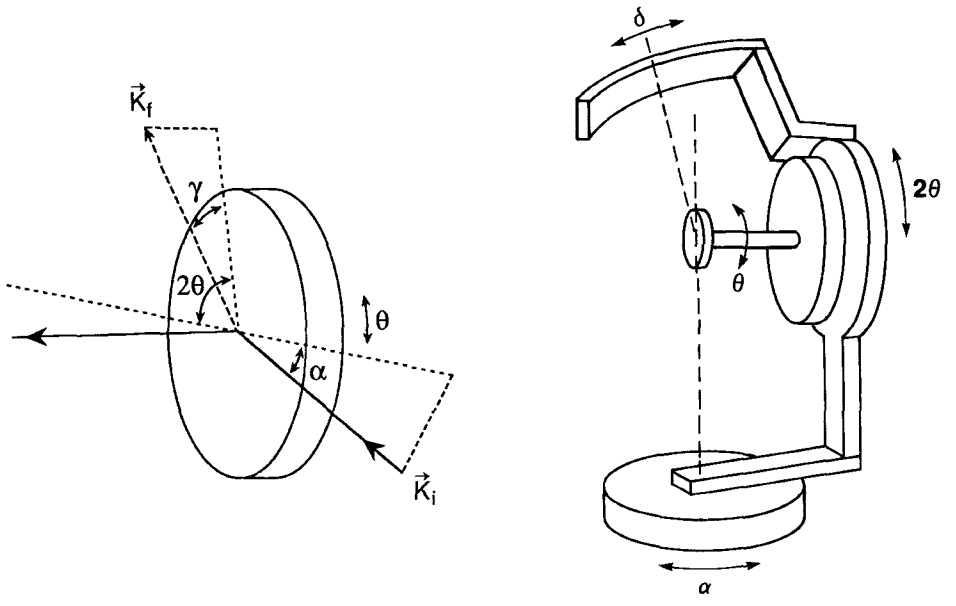

Figure 8. Schematic diagram of the experimental configuration usually employed for grazing incidence X-ray diffraction (GIXD) from surfaces (viewed from close to the incident beam direction). The orientation of incident and diffracted beams are indicated (*a*), with the typical mechanical configuration of a GIXD diffractometer (*b*).

of surface X-ray diffraction at grazing angles of incidence (GIXD) for the study of a wide variety of surface structural problems. New surface structures have been determined using *ab initio* techniques (for reviews see Feidenhans'l (1990) and Robinson (1990)) and surface phase diagrams have been explored. Depth-controlled GIXD structural studies have also been described (Dosch *et al.* 1986).

From a catalytic perspective we are currently interested primarily in two areas, the structure of single-crystal surfaces and the structure of adsorbed overlayers. The crystals of prime interest here are metals or oxides. The adsorbed layers might be metal on metal, metal on oxide, or molecular species such as CO, methane, or other more complicated hydrocarbons (depending on the nature of the species whose conversion is catalysed), on clean or metal-covered surfaces.

The utility of GIXD for surface crystallographic studies has been demonstrated by a number of results over the past few years from several synchrotron radiation centres, spanning applications to solid, liquid and polymer surfaces (for a review see Fuoss *et al.* (1990)). The determination of surface structure can now be pursued in direct analogy to conventional three-dimensional single crystal crystallography. An adequate set of (two-dimensional) reflection intensities is measured, corrected to yield structure factor moduli, and structure solution then attempted based on a Patterson map (calculated from the squares of the moduli). After successful derivation of a trial model, the associated model atomic coordinates can be optimized by conventional crystallographic least squares. A number of crystal surface structures have been solved by this *ab initio* approach (Feidenhans'l 1990, Robinson 1990), including complicated surface reconstructions such as InSb(111) 2×2 (Bohr *et al.* 1985) and Si(111) 7×7 (Robinson *et al.* 1986).

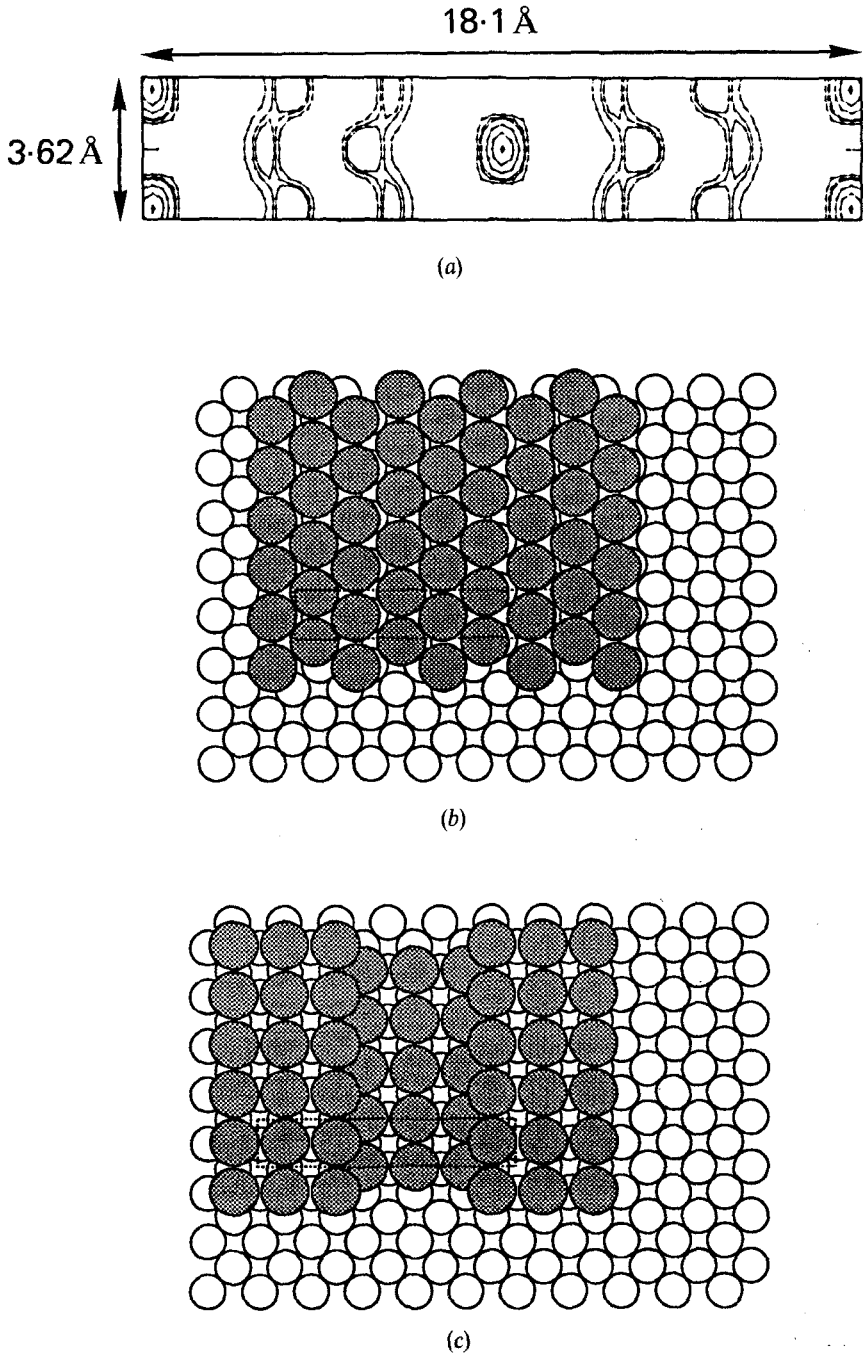

Figure 9. Patterson map (all positive density within the full unit cell is shown) computed from Bragg intensities measured from approximately a monolayer of Pb on the Cu (100) surface (*a*), and representations of the pseudo-hexagonal (*b*) and antiphase (*c*) domain structures that had previously been suggested as possible models for this system (Hoesler and Moritz 1986).

The potential for pursuing surface crystallography without the requirement of an assumed structural model represents a significant advantage over LEED. As an illustration, figure 9 shows a Patterson map computed from a set of reflection intensities measured from a (5×1) overlayer of Pb on a Cu(110) surface (Liang *et al.* 1989c). From LEED and Auger studies (Henrion and Rhead 1972), it is known that the (5×1) structure is formed on the Cu(110) surface at a saturated monolayer coverage. Auger results indicate that the coverage corresponds to about six Pb atoms per unit cell. Knowing that the lattice constant of Cu is 3·615 Å and the atomic radius of Pb is 1·75 Å, this number of Pb atoms per (5×1) unit cell would suggest some sort of a close packed structure. The Patterson map shows a number of distinct interatomic vectors but cannot be interpreted simply based on either of the two models (figure 9) previously discussed in studies using *I–V* curve fitting of LEED data (Hoesler and Moritz 1986).

In the context of catalysis, we are also interested in using GIXD to study the structures of adsorbed layers of low atomic number (Z) elements, such as O_2, CO and hydrocarbons. A back-of-the-envelope calculation indicates that for a dense monolayer of oxygen on a metal surface, a square millimetre of area contains a number of oxygen atoms equivalent to about a $7\,\mu^3$ crystal of the element. Clearly, without the intensity of the synchrotron source, X-ray diffraction experiments on these kinds of system would be completely impracticable. Such studies of low-Z species on surfaces tax even the modern generation of synchrotron X-ray sources, but a study of a prototypical O-(2×1) overlayer on a Cu(110) surface (Liang *et al.* 1985) (figure 10) indicates that such studies are feasible. Further work on more complicated molecules such as light hydrocarbons is certainly possible, particularly at the next generation of synchrotron facilities (such as ESRF and APS, see table 3).

Direct information on structure, that is the degree and character of long-range ordering of surface species, is not directly accessible using infrared, photoemission or absorption techniques. However, these methods can yield information on local structure, and, importantly, data on the orientation and bonding of surface states (Stohr 1985, Stohr *et al.* 1984). Synchrotron radiation has already played a substantial role in the development and application of several surface-sensitive local probes. In the future we expect that GIXD will be applied further to studies of phase transitions and to investigations under elevated pressures or *in situ* environments. The physics and phase behaviour of surface defect structures is a current focus for GIXD. Recent experiments have, for example, studied the roughening of a Cu(113) stepped surface (Liang *et al.* 1988) (figure 11). On the surface, the normal step–step distance is 4·24 Å. By measuring the temperature dependence of the step–step superlattice reflection, it was possible to determine the step–step repulsive energy (181 meV), the kink energy (7·4 meV) and the roughening transition temperature (620 K). Thermal excitations of defects on surfaces are relevant in a number of catalytic processes. In the case of Cu(113), such excitations are observed at temperatures less than one half of the melting temperature of bulk copper metal.

In common with diffraction, a key in applying absorption techniques to surface species is the attainment of sensitivity to the surface layer(s). Clearly, the simplest measurement of absorption by transmission is inappropriate (Lee *et al.* 1981), necessitating the development of detection techniques based on the reflected beam in grazing incidence geometry (Dring *et al.* 1989) (REFLEXAFS) or on X-ray fluorescence (Heald 1988, Stohr *et al.* 1985), or, of less practical use, electron photoemission, since the mean free path of a photoelectron in any but ultra-high vacuum conditions is small. A number of studies have been described (Stohr 1988).

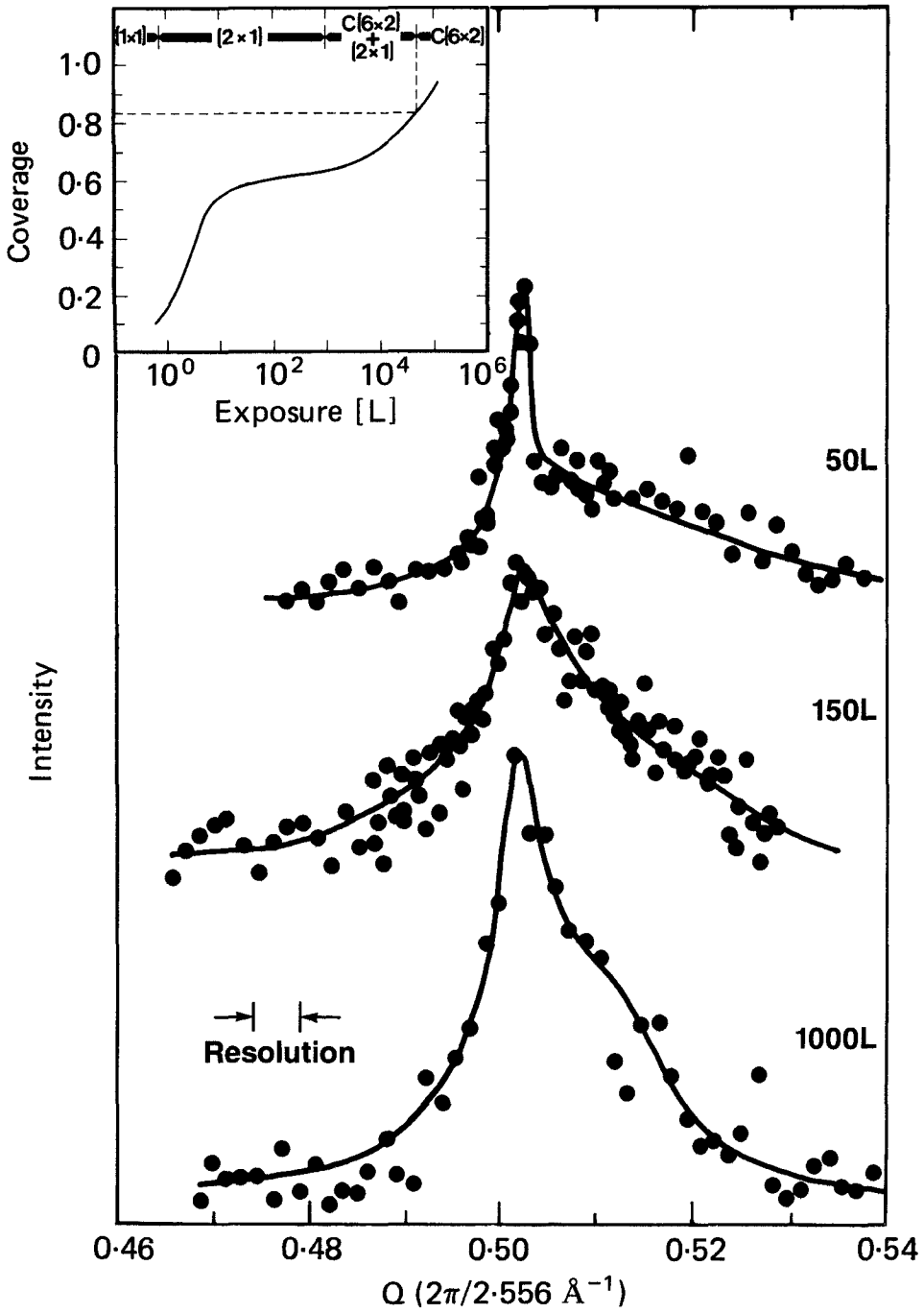

Figure 10. GIXD scans of the half-order superlattice reflection from the O(2 × 1)–Cu(110) surface layer at different oxygen exposures. The inset shows the coverage dependence of LEED patterns (Gruzalski 1984), 300 K $\lesssim T_s \lesssim$ 320 K.

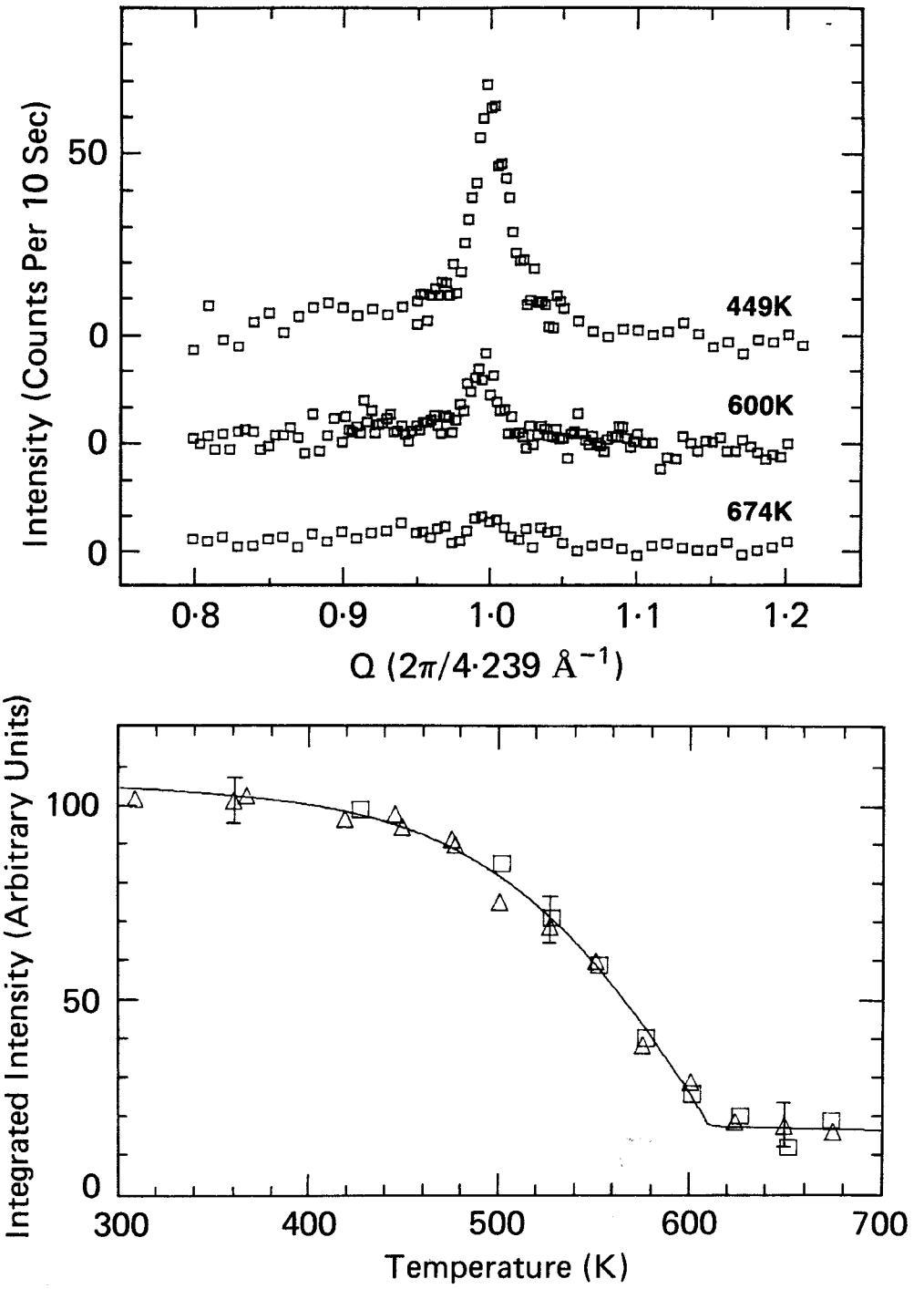

Figure 11. Intensity data measured in GIXD geometry for a step superlattice peak on the Cu (113) surface (upper), and variation with temperature of the integrated superlattice peak intensity (lower). The solid line is a theoretical fit (Liang *et al.* 1988).

5. Interfacial and boundary phenomena

Beyond well defined clean metal surfaces, the chemical and physical properties of a wide range of phase or grain boundaries and interfaces are of interest. In most catalytic systems such boundaries or interfaces are complicated, and little direct work has yet been reported. However, synchrotron X-ray diffraction methods have been applied to studying a number of interesting surface (Als-Nielsen 1987) and interfacial phenomena such as the phase behaviour of inert gases Kr (Birgeneau *et al.* 1981) and Ar (McTague *et al.* 1982, Nielsen *et al.* 1987) and CF_4 (Kjaer *et al.* 1982) adsorbed on graphite, smectic A ordering at the surface of a nematic liquid crystal (Als-Nielsen *et al.* 1982), phospholipid monolayers on a silicon wafer substrate (Seul *et al.* 1983), lipid monolayers (Kjaer *et al.* 1987), and species segregated as a layer(s) on a water surface such as the α-amino acid palmitoyl-(R)-lysine (Wolf *et al.* 1987), arachidic acid, $CH_3(CH_2)_{18}COOH$ (Kjaer *et al.* 1989), and lead octadecanoate, tetracosanoic acid and 1-eicosanol (Lin *et al.* 1988). The success of these studies imply that applications to systems of more direct interest in catalysis will be feasible.

As membrane technology develops, there will likely be increasing interest in the structural properties of thin films of which exterior and embedded surfaces can be examined by measurements of X-ray reflectivity at close to critical glancing angles, or by thin-film diffraction using grazing incidence geometry (Lim *et al.* 1987) or energy-dispersive techniques (Hart *et al.* 1987). For example, measurements of thin films of Co-doped iron oxide (Huang *et al.* 1987b), and investigations of superstructures at semiconductor interfaces (Akimoto *et al.* 1987, Mizuki *et al.* 1988, Robinson *et al.* 1988) have been described.

6. Dispersed catalytic metal particles

A wide variety of catalyst systems, such as those used in hydrogenation, dehydrogenation, reforming and Fischer–Tropsch chemistry involve metal atom or metal oxide dispersions on inert supports. Synchrotron X-ray research has figured prominently in the progress made in understanding the coordination and structural characteristics of such systems. High degrees of dispersion (with, correspondingly, relatively small metal or metal oxide cluster sizes) and low loading levels are generally involved. Conventional diffraction methods are, therefore, only of limited use. The application of other techniques can also be hampered by contributions from the support. Enhanced sensitivity to the target metal atoms in these systems may be achieved by exploiting the element-specific nature of X-ray absorption. As cited above, absorption (e.g. EXAFS) measurements have been successfully applied to a diverse range of supported catalysts. Additionally, changes in the atomic scattering factor occur in the vicinity of its absorption edges, giving rise to (element-specific) changes in the recorded diffraction patterns. The ability to select a desired narrow wavelength band (close to or far from the target absorption edge) from the broad incident X-ray spectrum is the basis for synchrotron X-ray diffraction studies that exploit this anomalous scattering.

The potential for anomalous scattering techniques (Ramaseshan and Abrahams 1975) was early recognized as being of particular promise for tackling the phase problem in protein crystallography (Guss *et al.* 1988, Harada *et al.* 1986, Karle 1989, Phillips and Hodgson 1980, Phillips *et al.* 1976, Rosenbaum *et al.* 1971). A recent study of $Zr_{0.81}Y_{0.19}O_{1.90}$ demonstrates neatly how anomalous scattering effects can be used to provide separate information about different species occupying crystallographically

equivalent sites (Moroney *et al.* 1988). The anomalous diffraction technique has also been applied to obtain the partial structure factors for liquids and amorphous materials (see for example Kortright and Bienenstock (1988)). It also proves extremely useful in studying metal dispersions on crystalline or amorphous supports (Liang *et al.* 1987, 1989a, b, Samant *et al.* 1988a, b).

Systems such as Pt–Al_2O_3, or Pt/Re–Al_2O_3 and related systems are the basis for commercial reforming catalysts. As a representative example successive measurements were made on a sample of 5 wt% Pt on an η-Al_2O_3 support as prepared, after reduction in H_2 at 220°C for 60 min, and following re-exposure to air (Liang *et al.* 1987). The diffraction profiles $1 \leqslant Q \leqslant 11$ Å^{-1} ($Q = 4\pi \sin\theta/\lambda$) were in each case scanned using an intrinsic Ge detector ($\Delta E \approx 200$ eV) at incident photon energies of 9 or 14 eV, and 99 eV below the Pt L_{III} edge ($\approx 11\,564$ eV). The changes in intensity that accompany the 3% change in the Pt atomic scattering factor are barely visible in the full patterns (figure 12). The difference patterns of the low-energy scan minus the scaled higher energy scan (that closer to the edge), however, are well defined and may be indexed completely on the basis of the face-centred cubic unit cell of Pt metal. The widths of the peaks indicate mean Pt particle sizes that range from around 5 Å in the near-amorphous structure observed for the as-received and air-exposed materials, to around 20 Å for the H_2-reduced sample.

The character of this system (which maximizes the Pt–Pt component in the Pt scattering) permits direct application of the differential anomalous X-ray diffraction (DAXD) technique. For a system in which the target atomic species (Pt) is an integral, coherent part of the substrate structure, the DAXD pattern would contain both Pt–Pt and Pt–substrate information. Although interpretation then becomes more complex, such studies will potentially afford insight into the Pt–substrate interaction.

Recently, these methods have been extended to bimetallic catalysts comprising Pt–Re on an SiO_2 support (Liang *et al.* 1989a, b) and Pt–Mo on a zeolite Y support (Samant *et al.* 1988a, b). For the Pt–Re system, differential diffraction patterns (DDP) were collected using X-rays with energies near the L_{III} edges of both Pt ($\sim 11\,564$ eV) and Re ($\sim 10\,535$ eV) on a series of samples containing from 1 wt% Pt–1 wt% Re to 10 wt% Pt–10 wt% Re. Figure 13 shows the total and differential (at Re edge) intensity curves of a 10 wt% sample. The Re DDP shows clearly that two forms of Re are present in this sample, hexagonal close-packed (h.c.p.) and face-centred cubic close-packed (f.c.c.). Since bulk Re has the h.c.p. structure, the appearance of the f.c.c. phase in this bimetallic catalyst was unexpected. The two metals Re and Pt are apparently interacting strongly in this system and the f.c.c. Re might result from some epitaxial intergrowth of the small particles. Similar experimental results for a 2·5 wt% sample are shown in figure 14.

One advantage of these types of X-ray structural studies on small particles is that the partial structure factors obtained can be conveniently modelled using the Debye equation (Liang *et al.* 1986, Warren 1969). The results of such calculations for the 2·5 wt% Pt–Re sample are shown in figure 14 for both Pt and Re DDPs. The measured Pt DDP agrees well with the calculated pattern of a 15 Å f.c.c. particle. To match the Re DDP, however, it was necessary to include both f.c.c. and h.c.p. structures in the model.

Anomalous X-ray diffraction measurements can thus yield valuable structural data on small catalytic particles on supports, complementing the local structural information afforded by absorption techniques such as EXAFS. These techniques may also be applied to *in situ* studies under close to real catalytic conditions (Samant *et al.* 1988a, b).

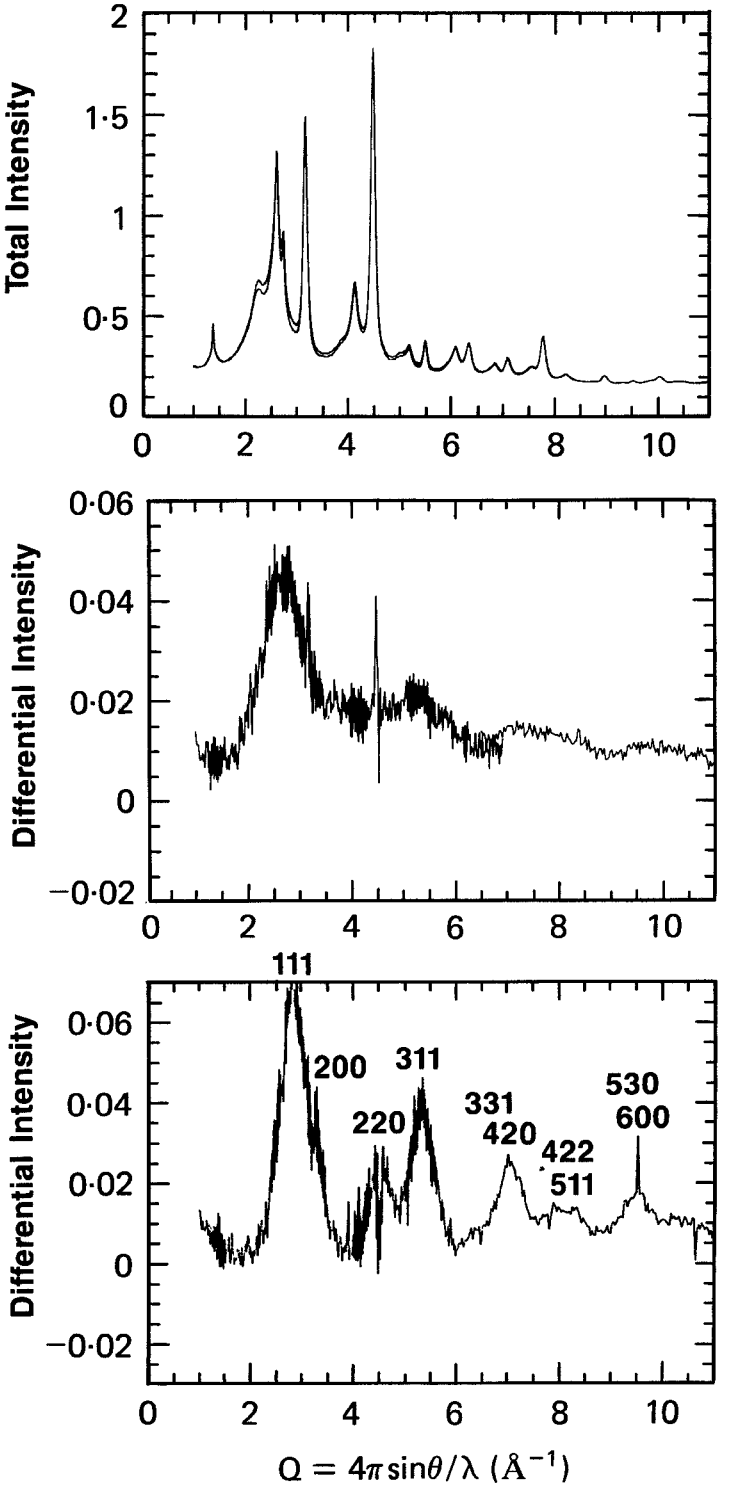

Figure 12. Total (*a*) and DAXD ((*b*) and (*c*)) profiles for a sample of 5 wt% Pt catalyst on η–Al_2O_3 both air-exposed (*b*) and after H_2-reduction (*c*).

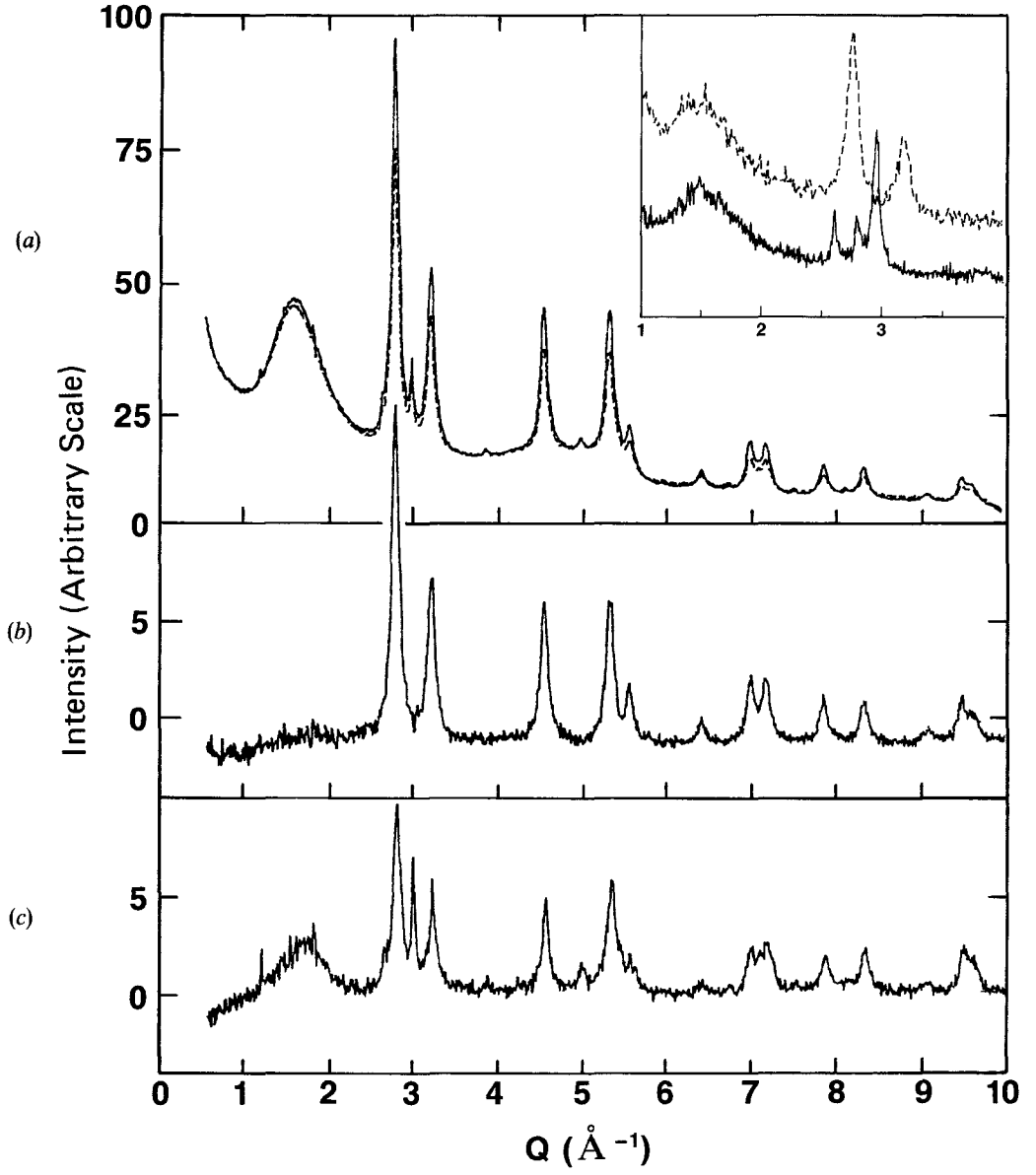

Figure 13. Powder diffraction profiles for a sample of 10 wt% Pt–Re catalyst on SiO_2. Total intensities (*a*) and differential intensities taken near the Pt L_{III} (*b*) and Re L_{III} (*c*) edges.

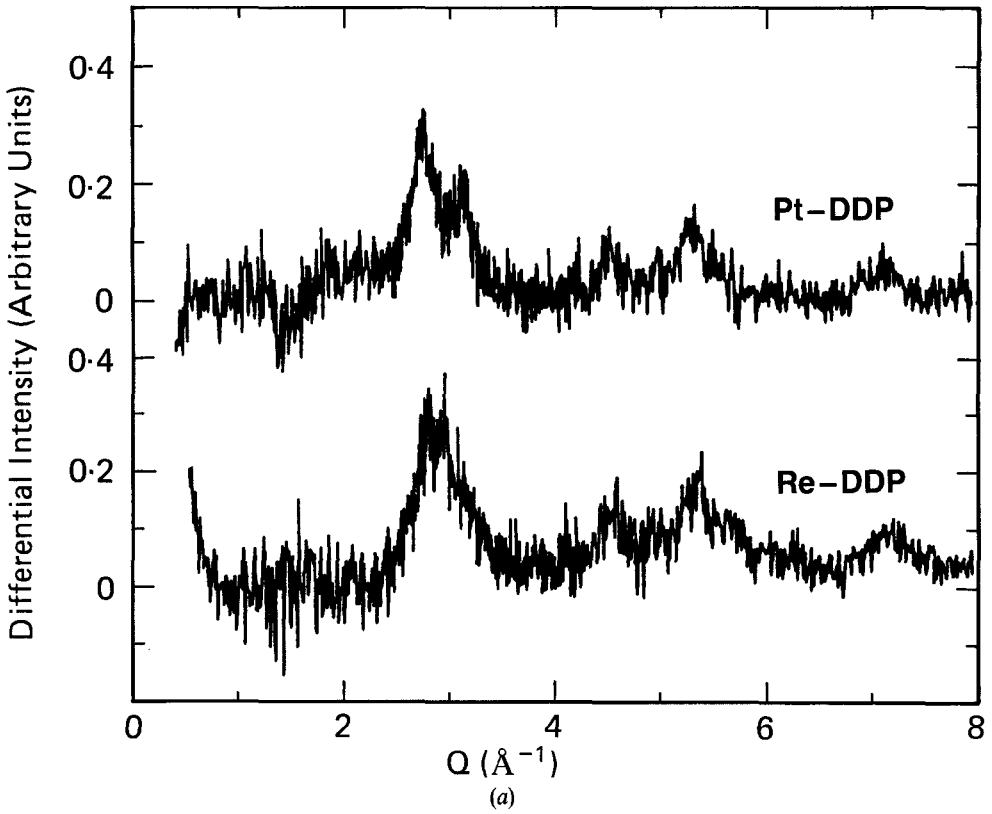

(*a*)

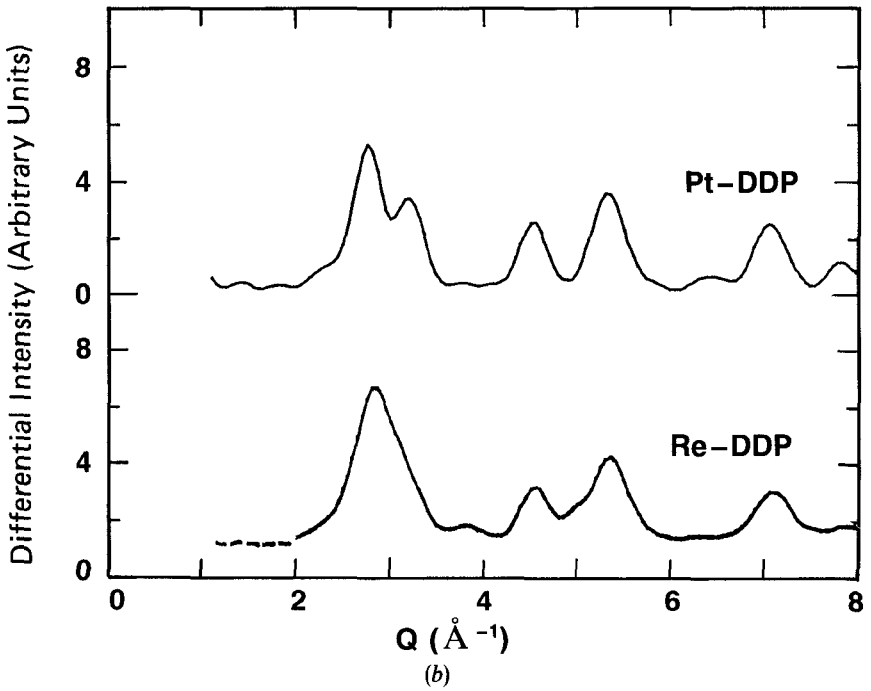

(*b*)

Figure 14. Differential anomalous X-ray diffraction (DAXD) profiles for a sample of 2·5 wt% Pt–Re catalyst on SiO_2 ((*a*) measured, (*b*) calculated).

7. Studies of bulk structure

Even for those heterogeneous catalysts for which activity is restricted to external surfaces, a detailed knowledge of bulk structure is generally the starting point for interpreting, for example, the adjustments that accompany interruptions at surfaces, or coordination rearrangements that occur in very small particles. In microporous catalysts such as zeolites, the bulk structure also plays a direct role in defining catalytic properties and for these and related crystalline catalyst systems conventional diffraction techniques can provide direct data on structural features of interest. Generally, materials of interest are polycrystalline (synthetic zeolites (Newsam 1986), for example, are almost invariably produced only as small particles, typically no larger than about 5 μm). Phase identifications and structure have, therefore, relied heavily on powder diffraction techniques. The synchrotron source provides significant enhancements both for powder diffraction experiments, and also enables new techniques to be applied to structure determinations based on polycrystalline samples.

7.1. *Powder diffraction*

The intensity, small source size and low divergence of the synchrotron X-ray source enable much higher resolution to be achieved for powder diffraction scans than is readily available in-house using focusing Bragg–Brentano geometry and a fine-focus X-ray tube source. In the high resolution experiment a narrow wavelength band is extracted from the incident continuous X-ray spectrum by a single or double perfect crystal monochromator (Si(111) or Ge(111) are commonly used, see table 4). The monochromatic beam is trimmed with slits or a collimator and is incident on a flat-plate or capillary sample.

The detection system for recording the powder diffraction pattern may be configured in a number of ways. In the typical arrangements shown schematically in figure 15, the diffracted beam acceptance angle is defined by slits (Parrish and Hart

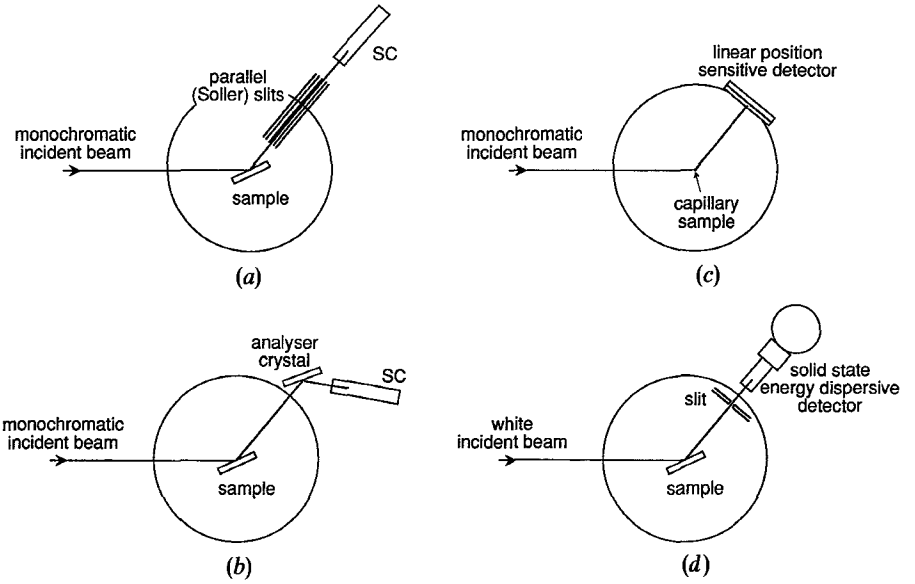

Figure 15. Schematic representations of the sample and detection configurations of four diffractometer arrangements used for powder diffraction experiments using synchrotron X-radiation.

1987, Parrish *et al.* 1986), by an analyzer crystal (Cox *et al.* 1983, Hastings *et al.* 1984), or in direct analogy to classical Debye–Scherrer geometry by a photographic film (Thompson *et al.* 1981) or linear position sensitive detector (Lehmann *et al.* 1988). Use of a single adjustable slit permits the resolution to be continuously tuned, although precise slit adjustment can be difficult to reproduce, and, more importantly, the region of the sample that is viewed by the detector is also determined by the width of the slits. At very fine resolution, only a small region of the sample is viewed, limiting count rates and exacerbating problems associated with obtaining a true powder average. Use of a Soller slit (Parrish and Hart 1987, Parrish *et al.* 1986) circumvents this limitation, but prevents simple resolution adjustment and has, in practice, an upper resolution limit. A diffracted beam monochromator crystal acts, in essence, like a perfect Soller slit, but with, in addition, energy selection which can help to reduce background due to sample fluorescence. For optimum signal intensities, the instrumental resolution could be matched to the sample characteristics via choice of analyzer crystal, although the choice of such crystals is currently limited (e.g. table 4) and frequent realignment can be tedious.

These are several ways that the high instrumental resolution readily obtained at the synchrotron X-ray source can be exploited in powder diffraction experiments. Improved instrumental resolution firstly greatly facilitates phase identification and definition (figure 16). Bi- or multi-phasic mixtures can more readily be decomposed into the contributing sets of PXD patterns. Variations in the peak widths from component to component can sometimes assist resolution (figure 16). This relatively routine use of synchrotron X-ray diffraction has, to date, been limited, although as access to beam time becomes more plentiful, further applications can be anticipated. As discussed above, powder diffraction experiments using a typical set-up enable the low-angle peak positions to be determined with good accuracy and precision. The application of automatic indexing procedures is, therefore, enhanced (Smith *et al.* 1987). With developments in computer modelling methods for structure determination, the unit cell size and symmetry information which is the result of a successful pattern indexing may, in itself, be sufficient to enable solution of certain framework structures (Deem and Newsam 1989).

Reduced peak widths, a more even background and/or greater source intensity permit identification of low-level impurity phases or studies of subtle superlattice ordering effects. Measurements on the zeolite silica-ZSM-12 on X13A indicated a doubling of the *c* parameter to 24·33 Å (Fyfe *et al.* 1990) (reflecting small adjustments in the zeolite framework geometry) compared with the first description of the ZSM-12 structure based on 'in-house' PXD data (La Pierre *et al.* 1985). Another example is provided by recent measurements on the zeolite (K, Ba)–G(L) at beamline X10B at NSLS (Newsam *et al.* 1989b). Measurements were made on a hydrated powder sample, and although refinement is incomplete encouraging agreement between observed and simulated powder diffraction profiles has been obtained (see figure 23 below). This material, for which the structure was first described in 1972 (Baerlocher and Barrer 1972), has a framework Si : Al ratio of unity. Although it was apparently not recognized earlier, long-range coherence to the Si–Al ordering scheme is required if Loewenstein's rule of Al–O–Al linkage avoidance (Loewenstein 1954) is obeyed. The model for the supercell (figure 17) requires a doubling of the *c* axis from 7·5 to 15 Å, although as the non-framework cation distribution is expected not to contribute to the superlattice peaks (which then arise from the scattering power difference between silicon and aluminium, coupled with slight readjustments in oxygen positions) they are anticipated

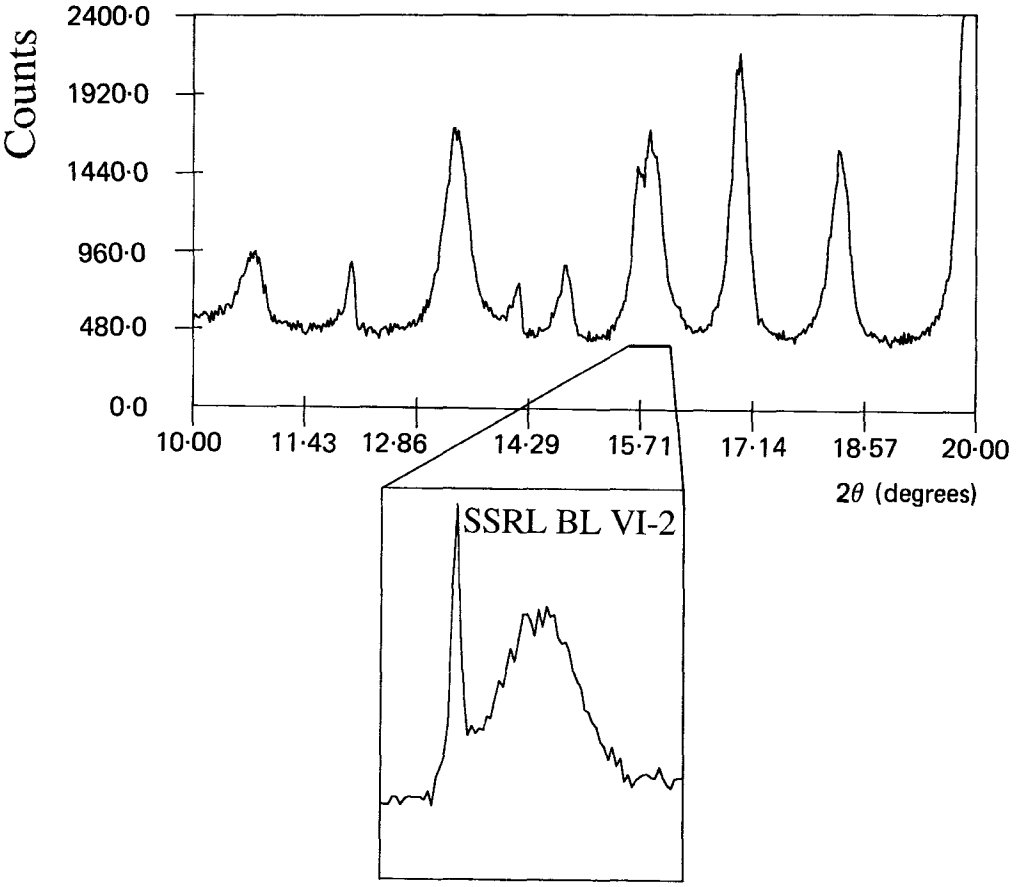

Figure 16. Sections of the powder diffraction profile (Cu Kα radiation, Siemens D500 diffractometer) for the product of a hydrothermal crystallization from a $Cs_2O.SnO_2.SiO_2.H_2O$ gel composition (Corcoran *et al.* 1989, Newsam *et al.* 1989a). The higher resolution synchrotron scan (inset) resolves the pattern into a mixture of both very sharp and broad peaks, indicating, in this case, the presence of at least two different phases.

to be weak, with a calculated maximum intensity in a resolved position of about 0·1% of the maximum. The region of the PXD profile from this material that includes the calculated position of the 131 superlattice reflection shows quite clearly a weak peak at the calculated position (figure 18). The width of the peak is comparable with that of the neighbour subcell reflections; the intensity is of the order anticipated on the basis of the superlattice model.

A reduced instrumental contribution to the line widths enables more precise evaluation of sample contributions to the measured peak widths (Huang *et al.* 1987a). A variety of factors may contribute to the measured peak shapes and widths, such as inhomogeneity (inter- or intracrystalline), strain, particle size effects or stacking disorder. Earlier studies have suggested that strain can have a pervasive effect on bulk zeolite properties (Treacy *et al.* 1986, 1988), although detection of strain fields in zeolite crystallites has so far been accessible only by careful measurements in the electron microscope. Particle sizes and shapes are also most conveniently examined in the electron microscope, but synchrotron X-ray powder diffraction can, complementarily,

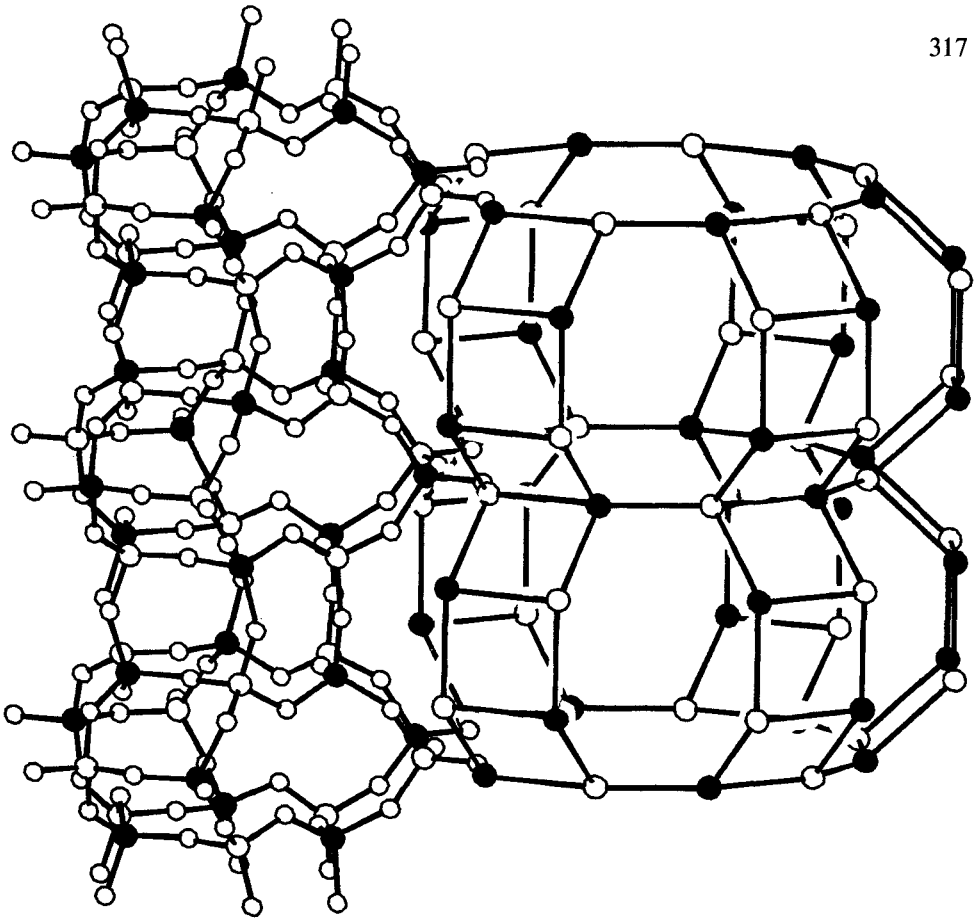

Figure 17. Ball and stick representation of the superstructure in the zeolite (K, Ba)–G(L) (Newsam *et al.* 1989b) (Si, O, open circles; Al, solid; non-framework species omitted). The full structure at left shows three cancrinite cages linked through hexagonal prisms. The shape of the lobed 12-ring channel is indicated on the right by straight lines connecting adjacent Si/Al sites and with oxygen atoms omitted). The requirement of the superstructure for the alternation of Si and Al can be tracked along the vertical direction.

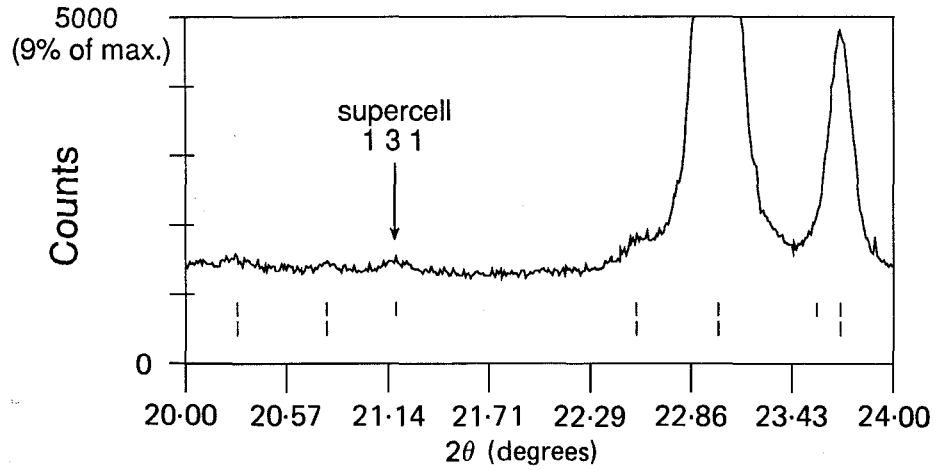

Figure 18. A small portion of the powder X-ray diffraction pattern of the zeolite (K, Ba)–G(L) measured on X10B, showing the presence of a weak superlattice reflection of approximately the relative intensity calculated based on the model shown in figure 17 (Newsam *et al.* 1989b).

reveal isotropic or anisotropic particle size broadening effects. Using an in-house instrument, such effects become significant only for sizes substantially less than 5000 Å (0·5 μm), but a much broader range of sizes can be measured using the higher instrumental resolution available readily at the synchrotron. Additionally, higher resolution permits sensible peak width measurements to be extended to a broader range of scattering angles, potentially improving resolution of size and strain effects, and enhancing definition of shape anisotropies. This is particularly valuable for more complicated structures such as those of zeolites. A portion of the PXD pattern of a natural ferrierite from the Lovelock deposit in Nevada (Rice 1989) compared with that measured from a synthetic material (figure 19) illustrates the influence of anisotropic particle size effects. The ferrierite structure is prone to planar defects of various types, but the major distinction between the two patterns in the region shown arises from the much thinner platelet habit of the synthetic sample. Quantitative analysis of the measured widths indicates a mean platelet thickness of some 1000 Å, consistent with direct observation in the electron microscope (Rice 1989).

Many zeolites are prone to stacking disorder. This stacking disorder is manifested in the corresponding powder diffraction patterns by altered peak intensities and by characteristic variations in the individual peak widths. Data from a series of materials in two distinct families of zeolites that are subject to stacking disorder (beta-type zeolites, and materials related structurally to faujasite and ZSM-20) illustrate the advantage offered by the higher resolution synchrotron X-ray diffraction data.

The hexagonal variant of the faujasite structure (generally termed Breck structure 6, labelled with the framework code *bss* here) was first recognized as a hypothetical structure type many years ago by Moore and Smith (1964), Breck (Breck and Flanigen 1968) and others. The structure is generated by replacing the inversion centres that relate successive faujasite sheets along the 111_{cubic} direction in faujasite (zeolite framework code FAU, see Meier and Olson (1987)) by mirror planes at the centres of the hexagonal prisms. The tetrahedrally connected supercages in the FAU framework are replaced by continuous channels along the $001_{\text{hexagonal}}$ direction, joined through supercages. The pore system continues to be 12-ring, three-dimensional in character. However, although recognized as a hypothetical structure for many years (Breck and Flanigen 1968, Moore and Smith 1964), no authentic example of this structure type had been reported. It has recently been found that the Mobil zeolite ZSM-20, although still a highly faulted example, contains extended regions of the hexagonal mode of stacking (Newsam *et al.* 1989b, Vaughan *et al.* 1989). The difference between the structure types is shown by the simulated powder X-ray diffraction patterns. The (first) single 1 1 1 peak for cubic faujasite is split into a triplet, the 002, 110 and 102 reflections for the hexagonal structure. For ZSM-20, in-house PXD data published recently (Ernst *et al.* 1987) do show a triplet of peaks in this region, although with relative intensities that differ significantly from those for the simulated hexagonal *bss*-framework (Vaughan *et al.* 1989b). Recent synthetic developments have now yielded materials that are structurally much closer to the pure hexagonal mode of stacking (Delprato 1989, Vaughan 1989).

A series of materials related structurally to faujasite, such as ZSM-20 (Newsam *et al.* 1989b, Vaughan *et al.* 1989), have been studied by high-resolution powder X-ray diffraction on X10B at a wavelength of 1·58 Å (Newsam *et al.* 1989a). This series (figure 20) includes examples of the pure cubic stacking (FAU) found in the mineral faujasite and related synthetic zeolites X, Y and so on (*a*), an example of a near-perfect hexagonal stacking sequence (*bss*) (*d*), and a range of materials representative of the

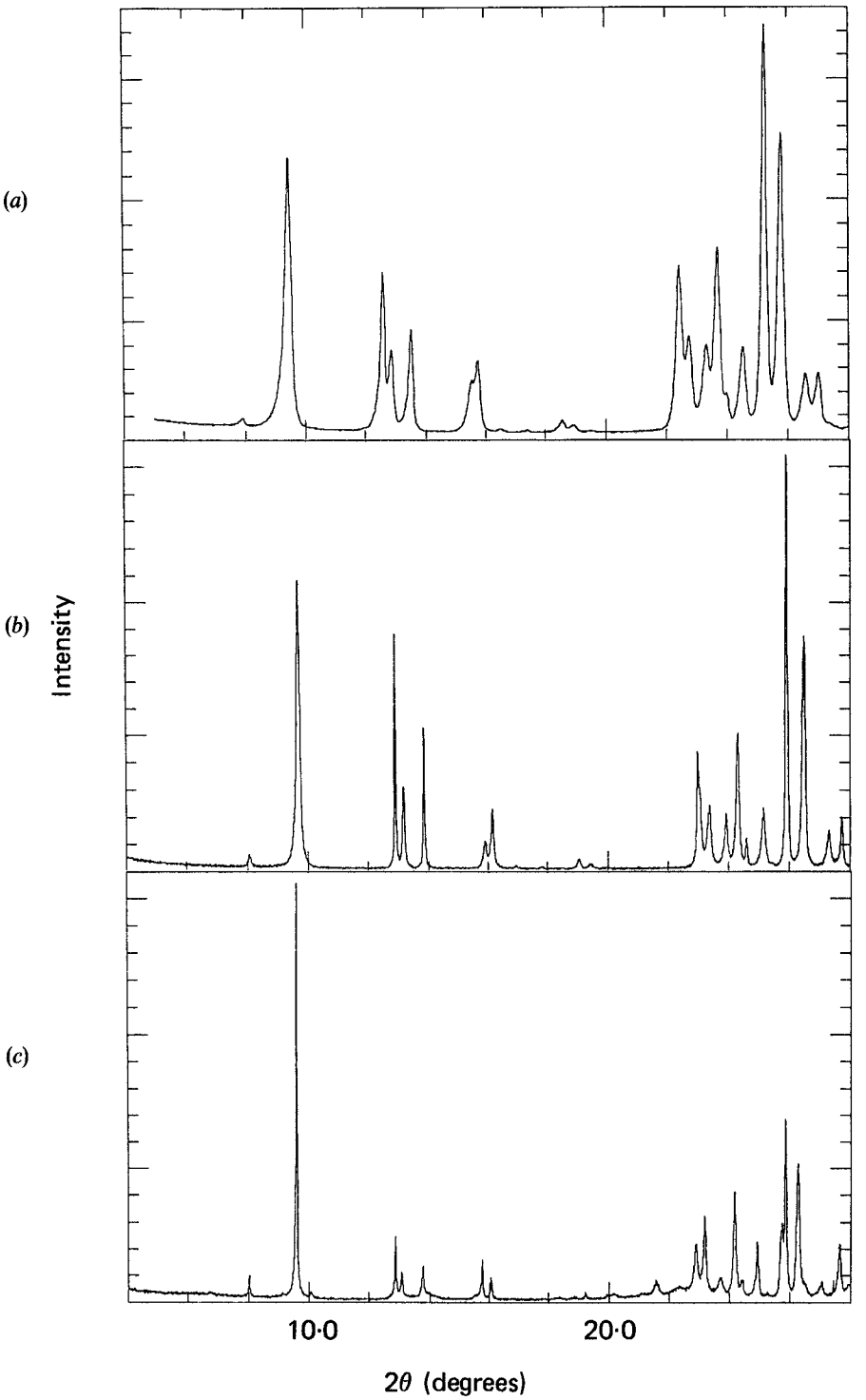

Figure 19. Powder X-ray diffraction data for two ferrierite samples, a synthetic material (top, Siemens D500 diffractometer data, and middle, X10B at NSLS) and a natural sample from the Lovelock deposit in Nevada (X10B—bottom) (Rice 1989).

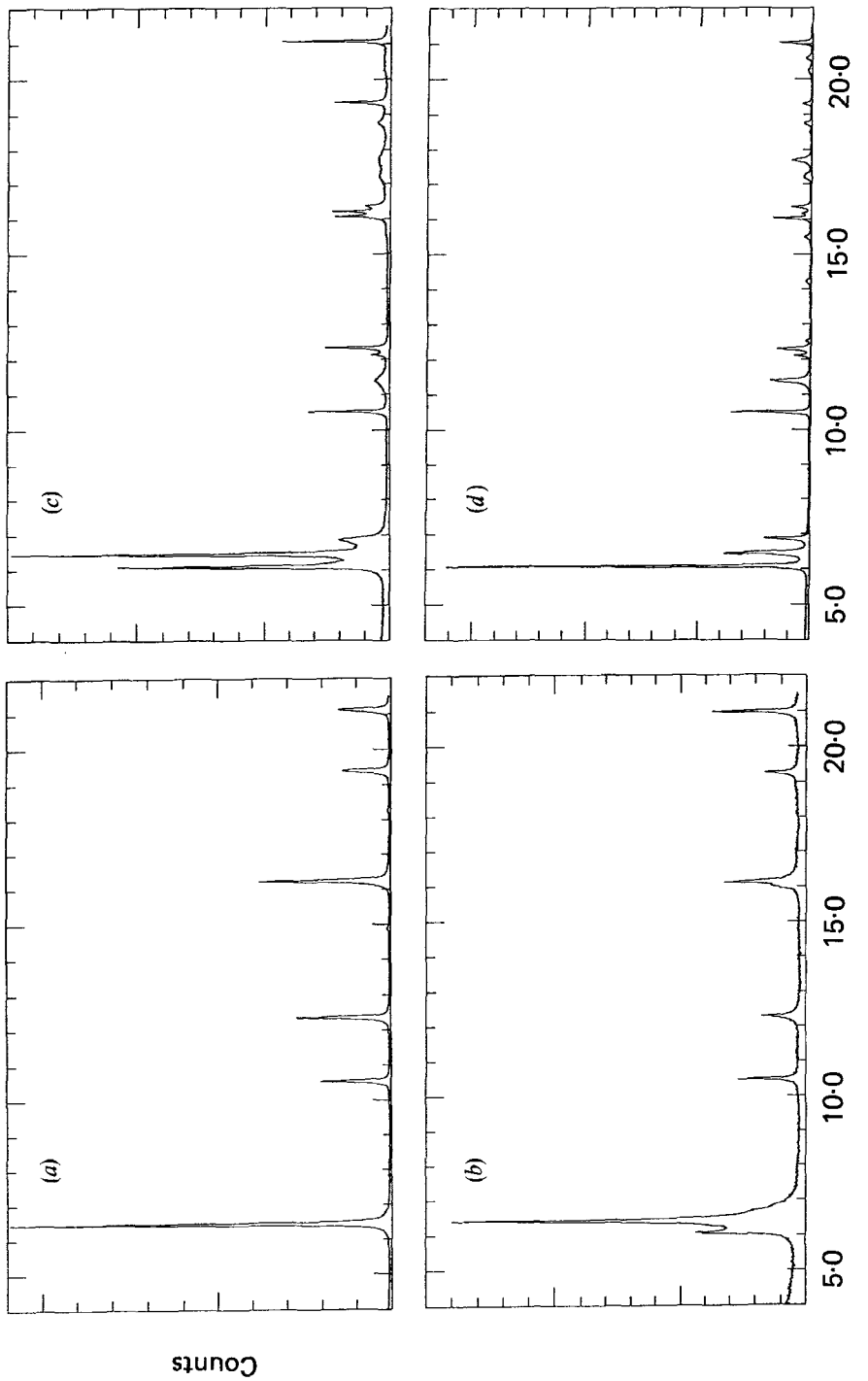

Figure 20. Powder X-ray diffraction data for four zeolites with, respectively, the cubic FAU framework (*a*), the bss–framework (a hexagonal variant (*d*)), and with varying degrees of intergrowth between the two end-member structure types ((*b*) and (*c*)).

phase field between these two end-member structure types (e.g. (*b*) and (*c*)). The character of the stacking sequences in these various materials is manifested by the distribution of intensities in the first singlet/triplet peak(s) (centred on $2\theta = \sim 6°$), by the relative intensities of the next group of peaks around $2\theta = 11°$, and by the relative widths of those peaks (such as the $103_{\text{hexagonal}}$ at $2\theta \simeq 11{\cdot}4°$) which are sensitive to the stacking disorder. The present data, combined with PXD pattern simulations (Treacy *et al.* 1989, 1990) and with parallel studies using in-house PXD and electron microscopy, give a definitive means of establishing the character of the stacking sequences, provide a self-consistent picture of the faulting in this system, and enable a classification of materials based on faulting characteristics.

Zeolite beta provides a near-extreme example of stacking disorder (Higgins *et al.* 1988, Newsam *et al.* 1988, Treacy and Newsam 1988). In common with the FAU-*bss* system, typical beta zeolites can be regarded as highly disordered intergrowths between two end member structure types. The first (A) has an ABAB... type stacking sequence of 12-ring pores (when viewed along the **a** or **b** directions). The other end member (B) has an ABC... type sequence when viewed along both of these directions (figure 21). Superficially, the system therefore has much in common with the FAU-*bss* one, although here the stacking disorder represents competition between 4_1 and 4_3 stacking vectors rather than between inversion centres and mirror planes. End member A has an uninterrupted 4_1 (or 4_3) type of stacking; end member B has recurrent alternation $4_1 4_3 4_1$. In this case neither end member structure has apparently yet been synthesized. This is unfortunate, because the A end member would occur in two enantiomorphic (optical isomer) forms with chiral pore systems and with potential, therefore, for use in enantiocatalysis or enantio- (optical isomer) separations.

Materials extracted from a wide range of synthesis conditions and compositions, however, have stacking sequences that represent close to random intergrowths between the modes of stacking. For these materials, the higher instrumental resolution afforded by synchrotron powder X-ray diffractometers is generally of little value; the PXD

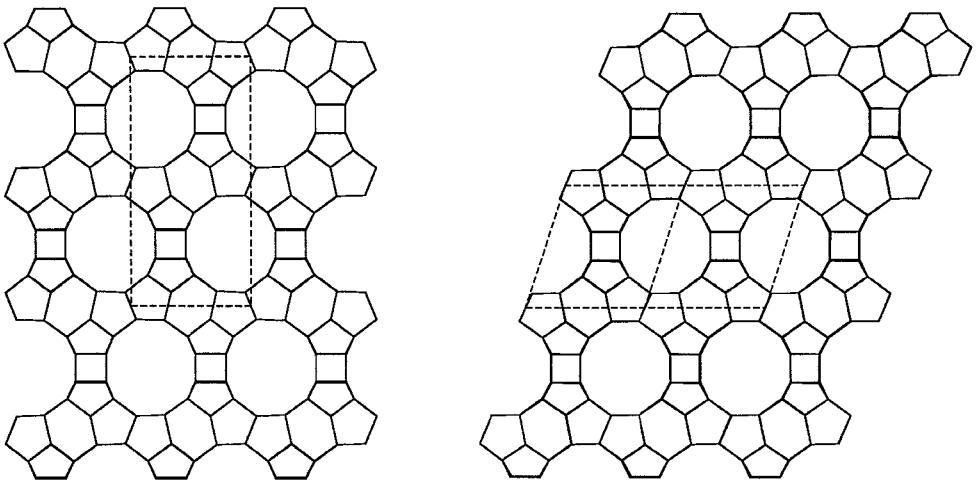

Figure 21. Representations of the bea and beb framework structures (drawn in projection as straight lines connecting adjacent T-sites; T = tetrahedral species, Si or Al) of which zeolite beta can be regarded as a disordered intergrowth (Higgins *et al.* 1988, Newsam *et al.* 1988, Treacy and Newsam 1988).

patterns comprise both sharp and broad lines, although the peaks that are expected to be sharp on the basis of the model of the faulting behaviour, such as 004, 302 and 008, (Higgins *et al.* 1988, Newsam *et al.* 1988, Treacy and Newsam 1988), are generally broader than the instrumental component. This reflects that the effective crystalline size along the stacking direction is generally relatively small, less than 600 Å. Nevertheless, studies of a large number of samples using synchrotron X-ray diffraction do demonstrate some differences from one preparation to the next. In a small number of cases, the sharp peaks have quite narrow widths (figure 22). Even in these cases, however, there is no development of definition in the remainder of the powder diffraction profile, demonstrating that the character of the pore stacking arrangement is essentially unchanged.

With higher resolution powder diffraction data the possibilities for *ab initio* structure solution are enhanced. When a good set of intensity data from a single crystal is attainable, structure solution is often straightforward, and excellent definition of structure can be obtained. In principal, an approximation to the full set of three-dimensional intensity data can be extracted from the powder diffraction profile by decomposing the pattern into a series of discrete integrated intensities for each of the contributing reflections. For conventional equipment, such data has two intrinsic limitations. Firstly, the data generally provide a 'weak' data set with limited signal-to-noise and hence only limited definition of the structure factor moduli. Secondly, and more critically, the peak overlap that occurs to a progressively more marked

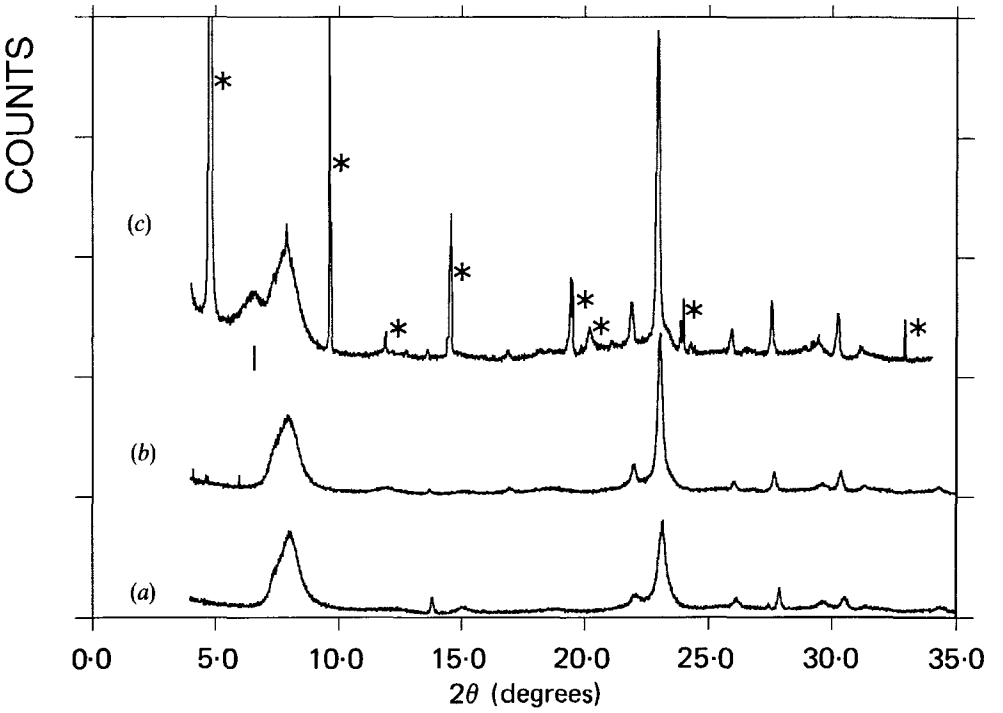

Figure 22. Powder X-ray diffraction profiles for three different samples of zeolite beta measured using a Ge (111) analyser crystal which provides an effective instrumental resolution (full width at half maximum) of ~0·02°. Impurity lines that contaminate the topmost pattern are marked (Newsam *et al.* 1989c).

degree at successively higher Bragg angles prevents unique determination of the intensities of each of the contributing reflections (see figure 19, for example). Relatively simple simulations of the effects of peak overlap on the definition of the structure factor moduli illustrate that *ab initio* solutions using in-house diffraction capabilities (see for example Le Bail *et al.* (1988) and Rudolf *et al.* (1986)) become impracticable in the more complicated cases. Improved instrumental resolution significantly enhances the quantity of intensity data which can be reliably determined and hence improved the possibilities for success.

Examples of *ab initio* structure solutions based on synchrotron PXD data which have already appeared include the structures of α-$CrPO_4$ (Attfield *et al.* 1986, 1988), the clathrasil Sigma–2 (McCusker 1988), UPd_2Sn (Marezio *et al.* 1988) and lead oxalate, PbC_2O_4 (Nørlund Christensen *et al.* 1989) that were each determined from PXD data collected on beam line X13A at NSLS (Cox *et al.* 1986). The structure analysis procedure typically involves indexing the peaks in the PXD profile, followed by decomposition into individual peak intensities. The decomposition (deconvolution) is conveniently accomplished using a full profile fitting procedure in which the unit cell and profile parameters, and the reflection intensities are the independant variables (with constraints on the appropriate intensity sums to prevent instabilities when substantial overlap occurs (Pawley 1981)). Direct methods or Patterson techniques can then be applied to the structure factor moduli derived from the decomposed intensities in an attempt to derive an (approximate) initial structural model. These structure solution techniques are continually being updated and further refined, facilitating applications to data from powder samples. Computer modelling methods which can assist the structure determination process are also being actively pursued (Deem and Newsam 1989).

Once an approximate structural model is available, the associated atomic coordinates can be optimized by integrated intensity refinement, or Rietveld (full-profile analysis) procedures (figure 23). Where peak overlap occurs, improved instrumental resolution entails an increased information density in the diffraction profile, and an increase in the amount of number of observed data enables a larger number of structural parameters to be meaningfully varied in the structure refinement. Rietveld analysis techniques can therefore be applied to refinements of more complicated structures. In addition to a number of model refinements on known structures (Cox *et al.* 1983, Thompson *et al.* 1987, Will *et al.* 1987b, 1988), Rietveld analyses of a number of topical systems have been described, including $MnPO_4.H_2O$ (in which, remarkably, hydrogen atom positions were determined and refined (Lightfoot *et al.* 1987), the mixed metal oxides $Ca_{0.75}NbO_6$ (Hibble *et al.* 1987), $LaMo_5O_8$ (Hibble *et al.* 1988), $SrNb_8O_{14}$ (Köhler *et al.* 1988), $Al_2Y_4O_9$ (Lehmann *et al.* 1987) and TiNF (Wüstefeld *et al.* 1988) and I_2O_4 (Lehmann *et al.* 1987), in addition to those studies previously mentioned.

A number of zeolite structures have also been refined, including those of ZSM-11 (Fyfe *et al.* 1989, Toby *et al.* 1988), and silica-ZSM-12 (Fyfe *et al.* 1990) where, in both cases, the previously reported atomic coordinates had been optimized solely by distance least squares optimization (Kokotailo *et al.* 1978, La Pierre *et al.* 1985). The ZSM-11 studies illustrate that the high instrumental resolution provided by synchrotron powder instrumentation does not necessarily enable a straightforward structural interpretation. The initial report described a complete structure refinement at 298 K (Toby *et al.* 1988), although the subsequent analysis (Fyfe *et al.* 1989) determined that the structure was temperature-dependent in the range 263–363 K,

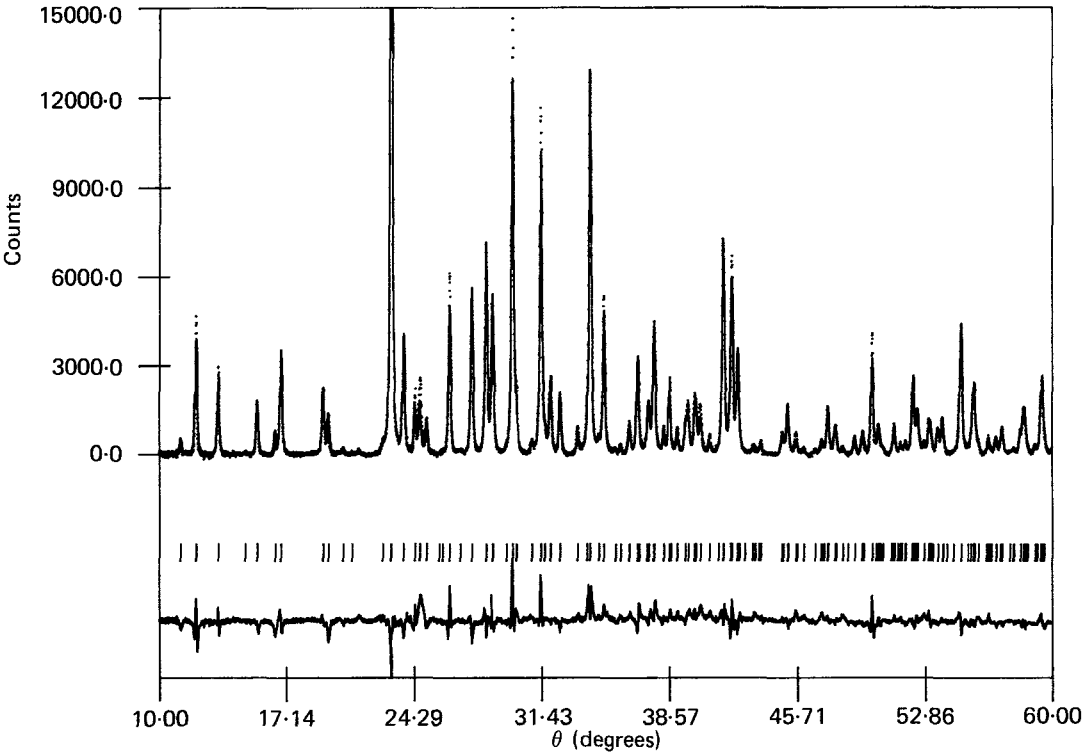

Figure 23. Observed (dots), calculated (continuous line) and difference (lower) profiles based on preliminary Rietveld refinements (for the subcell structure) of powder X-ray diffraction data from the hydrated zeolite (K, Ba)–G(L) measured on X10B.

preventing an unambiguous interpretation of the room temperature data. The studies demonstrate well the complex structural problems which zeolites frequently present. Other recent and interesting zeolite applications have been the complete structure determinations of zeolite Y containing cadmium sulphide (Herron *et al.* 1989) and cadmium selenide (Moller *et al.* 1989a) clusters.

Anomalous scattering effects discussed earlier in the context of dispersed metal particles may also be exploited in high-resolution powder diffraction experiments (Will *et al.* 1987a). The use of differential anomalous X-ray diffraction has already been applied to differentiating between different species occupying crystallographically equivalent sites (Moroney *et al.* 1988) and such experiments may assist, for example, the structural characterization of hetero-substitutions at relatively low absolute concentrations in zeolite framework sites (figure 24).

Accessing the high intrinsic resolution afforded by the synchrotron X-ray powder diffractometer places significant constraints on the quality of the samples. Firstly, particle size broadening effects become significant at larger particle sizes. In the ZSM-11 study cited above (Toby *et al.* 1988), for example, an apparent sample contribution gave peak widths a factor of two greater than the effective instrumental resolution, leading to an estimated mean particle dimension of 0·4 μm. To obtain the full potential resolution, $\Delta d/d = 0{\cdot}004$, one would require particles larger than about 1 μm. The experiment thus imposes rather limited boundaries on the particle size, since with particles much larger than a few micrometres, a true orientational or powder-averaged distribution becomes difficult to obtain.

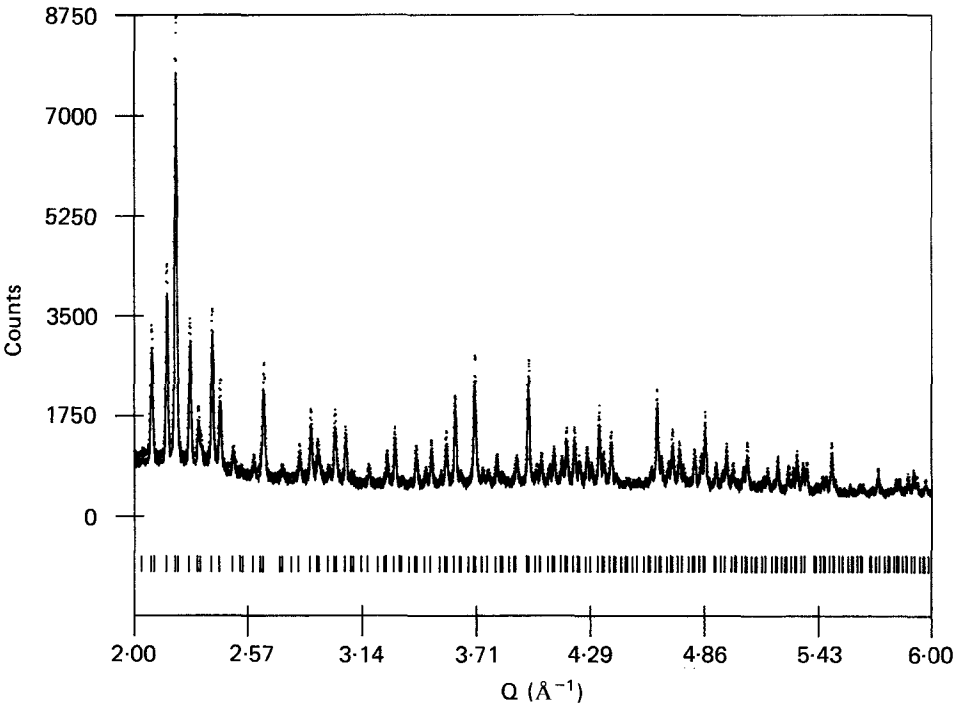

Figure 24. Powder X-ray diffraction data measured from an iron-containing zeolite Y, $Na_{60}Fe_{20}Al_{40}Si_{132}O_{384}.nH_2O$ at incident X-ray energies of 7103 eV (dots) and 6813 eV (continuous line), respectively 10 and 300 eV below the Fe K absorption edge (measured at 7113 eV).

7.2. *Single-crystal diffraction*

Single-crystal diffraction experiments can exploit each of the special features of synchrotron X-radiation. The source time structure has been exploited, for example, in diffraction studies of silicon during pulsed laser annealing (Larson *et al.* 1982). The low source divergence provides high resolution also in the single-crystal case, enabling studies of strain or mosaic (Kvick 1988), or, indeed, of how the mosaic character evolves with varying conditions (see below). The source brightness permits subtle incommensurate or superlattice structures to be examined (Moncton *et al.* 1987). Anomalous scattering effects can, as above, be exploited (see for example Lee *et al.* 1989, Sakamaki *et al.* 1984) and the continuous character of the source, coupled with a high ring energy (such as the 5·5 GeV facility at CHESS, see table 3) can provide intense beams of X-rays of short wavelength, $\leqslant 0{\cdot}5$ Å. In this spectral range, the effects of multiple scattering which give rise to extinction effects are minimized and essentially extinction-free measurements can, therefore, be performed. In a feasibility study, over 7000 reflections were collected at 0·32 Å at CHESS from a crystal of size $\simeq 100$ μm of hexamminechromium hexacyanochromate. Full structure refinement gave an excellent residual, $R = 0{\cdot}028$, and yielded good X–X deformation density maps (Nielsen *et al.* 1986). The polarized character of the source also permits exploitation of X-ray dichroism. The absorption cross-sections and hence the anomalous scattering factors for an atom in a site symmetry lower than tetrahedral depend on the polarization of the incident light. Measurements on potassium tetrachloroplatinate(II) at close to the Pt L_{III} edge have demonstrated this effect (Templeton and Templeton 1985, 1989).

The extreme brightness of the synchrotron radiation source facilitates studies of samples at high pressures in a diamond-anvil cell. Such samples are intrinsically small (10 nl–0·1 pl) because the sample chamber is a small circular hole (about 75 μm diameter × 20 μm) in a thin metal gasket between two flat diamond faces. Single crystal diffraction experiments on hydrogen at pressures of up to 26·5 GPa (Mao *et al.* 1988), and on sodium zeolite X at pressures of up to 3·2 GPa (King and Newsam 1989) have been performed.

The earlier discussion of particle size broadening effects on the powder diffraction peak widths leads naturally to the next example of synchrotron X-ray diffraction methods. Although for effective particle sizes less than some 0·5 μm particle size broadening is not observed in a typical in-house experiment, the greater instrumental resolution at the synchrotron imposes greater demands in terms of sample perfection, and for resolutions as typically configured, particle sizes larger than 1 μm are required.

Some years ago now it was demonstrated that crystallites with volumes of the order of a few cubic micrometres (1 $\mu m^3 = 1$ fl or 10^{-15} l) were measurable individually given the brightness of today's synchrotron X-ray sources. Although these first measurements (Bachmann *et al.* 1985, 1983, Eisenberger *et al.* 1984, Hoeche *et al.* 1986, Newsam and Vaughan 1985) demonstrated that sufficient X-ray flux was available, microcrystal diffraction experiments pose other difficulties, such as manipulating and mounting tiny particles, and defining their orientation on the diffractometer at the synchrotron. A SEM micrograph of a 12 μm crystal of zeolite X glued (with some difficulty) to the end of a 40 μm diameter solid glass fibre (figure 25) provides a basis for illustrating progress that has been made in these other areas (Newsam *et al.* 1989a). This type of mount is typical for conventional single crystal diffraction experiments. By carefully minimizing the instrumental background (including the large contribution

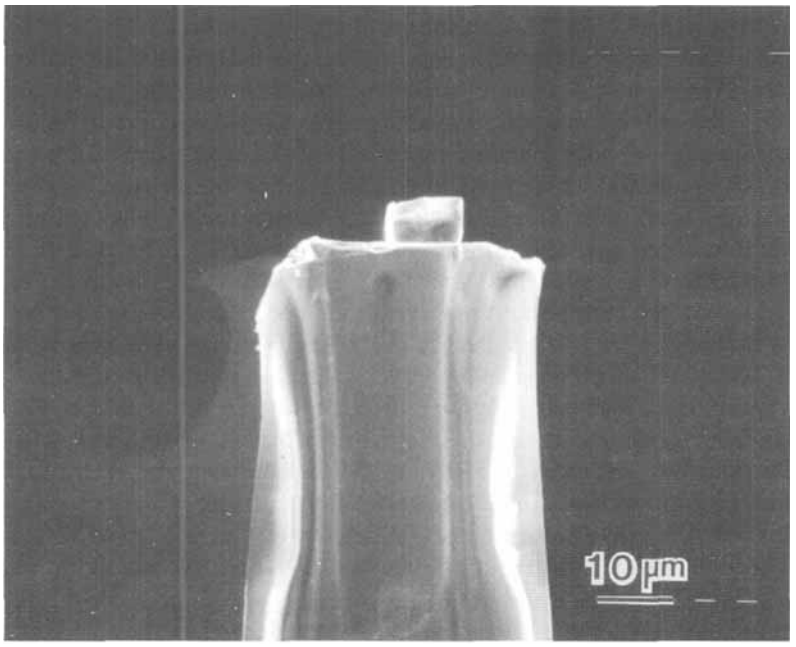

Figure 25. SEM micrograph of a 12 μm zeolite X crystallite mounted on a 50 μm diameter solid glass fibre (Newsam *et al.* 1989a).

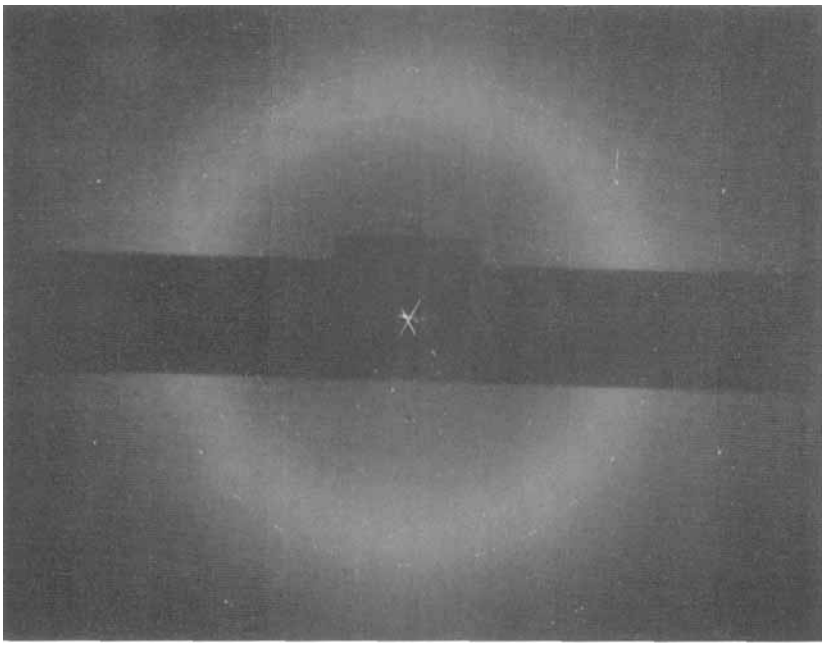

Figure 26. A 120 s rotation exposure recorded on beamline X10A from a 12 μm zeolite X crystallite(s) similar to that shown in figure 25. Sharp diffraction spots are readily discerned. The diffuse halo represents scattering from the tip of the glass fibre mount (Newsam *et al.* 1989a).

from air scattering) a rotation exposure was obtained from a crystal (figure 26). The ability to record rotation exposures is significant for, given the typically small crystallite rocking curve widths, an extremely fine mesh (with a correspondingly long search time) would be required for a random search for reflections in 2θ–χ–φ space. Once an adequate subset of reflections has been centred, unit cell and orientation matrix optimization can be performed in the usual way. The sharp bright diffraction spots from the crystal(s) are manifested by their occurring with mm symmetry on the rotation exposure. A large number of such spots are seen; measurement of the reflection coordinates on the rotation exposure then reduces the problem of defining setting angles to the (tractable) one of scanning a single circle, ϕ. The diffuse halo that is apparent is scattering from the small amount of the glass fibre that was in the beam. Were even a few centimetres of air to be present in the beam, the resulting background would be sufficient to swamp the features of interest evident in this exposure.

It actually proves quite difficult to deal with microcrystals using fibres this large. Current mounting methods use hollow glass fibres that taper to a point of less than 1 μm. Crystals that are $\geqslant 5$ μm in size may now be selected and mounted with an excellent success rate (Newsam *et al.* 1989a). Figure 27 shows a SEM picture of a 6 μm crystal of zeolite A glued to one of these fibres. In this case, the edge of the cube contains approximately 2500 unit cells. Well defined diffraction spots from a similar 7 μm sample were clearly evident on a rotation exposure. It is important to note that the widths of the diffraction events in crystal rotation are at a minimum some 0·02° (figure 28). The film background is being accumulated over a full 360°, and so the signal to background ratio on the rotation exposure is up to some 40 000 times worse than would be accessible using the detector. Thus, today's synchrotron sources provide

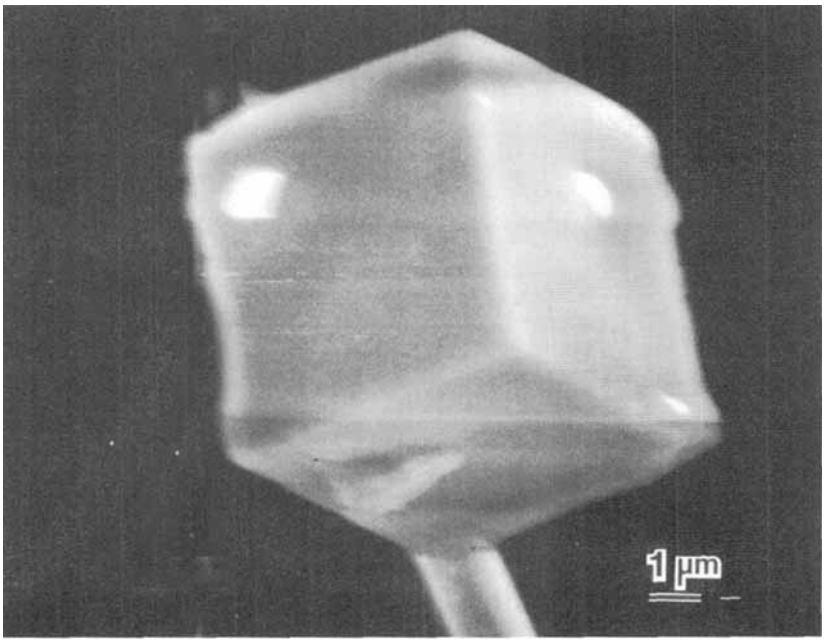

Figure 27. SEM micrograph of a 6 μm crystal of zeolite A (some 2500 unit cells on an edge) glued to a hollow glass fibre that tapers to a point of < 1 μm (Newsam *et al.* 1989a).

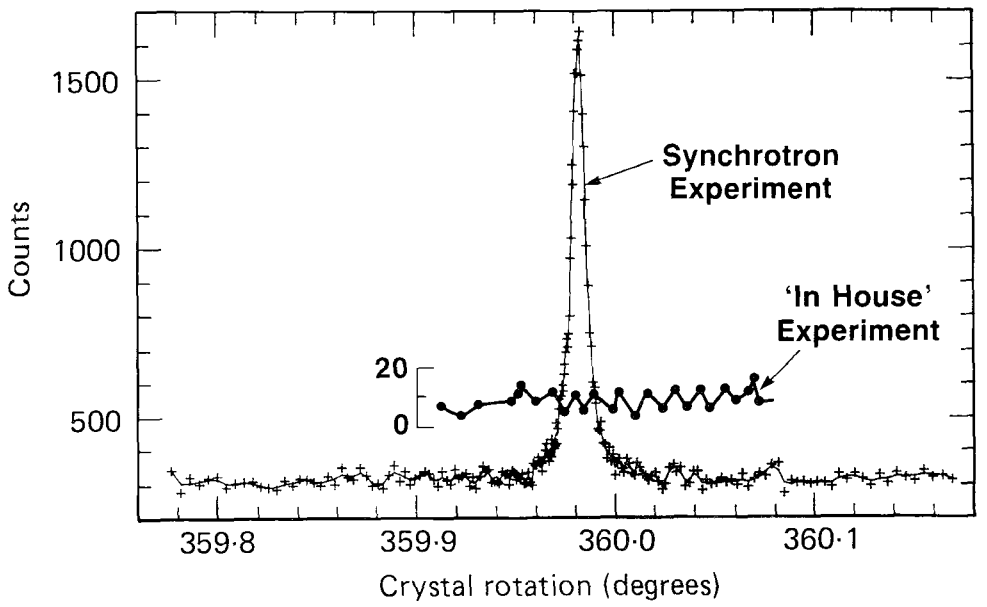

Figure 28. Single reflection profile $(0\,1\,4)_{subcell}$, measured on the Exxon beamline X10A at the NSLS, Brookhaven from a 7 μm zeolite crystallite similar to that shown in figure 25 (comparable 'in-house' data are also shown) (Newsam *et al.* 1989a).

sufficient flux to study micrometre size particles individually (Rieck *et al.* 1988). Methods for manipulating, mounting and defining the orientation of such microcrystals are in place (in a number of instances, the data on unit cell dimensions and symmetry provided quite readily by microcrystal diffraction experiments can enable further treatment of in-house single crystal (Leonowicz *et al.* 1985) or powder diffraction data (Corcoran *et al.* 1989)). A last hurdle is to obtain reliably and reproducibly totally internally consistent data sets accumulated over several hours or days at the synchrotron. This is not an easy problem and one that several groups have wrestled with. Largely for this reason, the number of successful small molecule or inorganic single crystal diffraction studies remains quite small. Notable are the studies by Nielsen *et al.* (1986) on hexamminechromium hexacyanochromate, by Ohsumi *et al.* (1987) on lillianite, by Kupcik *et al.* on a number of organic systems (Kupcik 1988), by Andrews *et al.* (1988) of a piperazine silicate (notably using area detector data, see below) and model studies of CaF_2 (Bachmann *et al.* 1985, Hoeche *et al.* 1986, Rieck *et al.* 1988), ruby (Al_2O_3) (Newsam and King 1987), cuprite (Cu_2O) and ruby (Kirfel 1988), and a borosilicate sodalite (Kvick and Rohrbaugh 1988). These studies demonstrate that this problem of stability should, in general, prove to be solvable. Clearly, were precise and complete data sets obtainable routinely from single crystallites in powder samples, there would be much less incentive for resorting to powder diffraction techniques for structure refinements and solutions.

When microcrystal diffraction experiments were originally proposed, questions as to sample heating, gross radiation damage, or damage of the sample mount in the finely focused very intense X-ray beam were raised. Experience has shown that many of these factors are not of major significance, although in zeolite materials degradation has been observed to occur over a relatively long half-time (several weeks) after X-ray exposure at the synchrotron. Problems associated with the quality of materials which occur only as very small particles have also been noted (Andrews *et al.* 1988, Harding 1988). Certainly, several materials do occur only in highly faulted or poorly crystalline form, although many of the systems that we have investigated to date (Eisenberger *et al.* 1984, Newsam and King 1987, Newsam *et al.* 1989a, Newsam and Vaughan 1985) have yielded crystallites with acceptable scattering characteristics.

One way of circumventing some of the problems associated with temporal fluctuations in the synchrotron X-ray source is to use an area detector where a large number of data are accumulated simultaneously, providing intrinsic internal scaling. Area detectors have been in regular use for protein crystallography for a number of years (where the requirement for precision on the measured intensities is more relaxed) and studies of a small number of inorganic and organic structures have been completed (Andrews *et al.* 1988). A variety of next-generation area detectors based on multi-wire technology, charge-coupled devices (CCD, with or without an image intensifier) or imaging plates are under development (see for example Amemiya *et al.* (1988), Milch *et al.* (1982) and Prieske *et al.* (1983)) and promise substantial improvements for single-crystal synchrotron X-ray diffraction experiments in the near future.

Laue diffraction (where the various planes in the (stationary) crystal diffract those wavelengths from the continuous incident spectrum for which Bragg's law is satisfied in the given orientation) simultaneously exploits both the brightness and the white character of the synchrotron X-ray spectral distribution, and, in this combination, intensity data may be accumulated on an extremely short time scale. A unique volume of reciprocal space is covered by recording data, typically on film packs, at a small

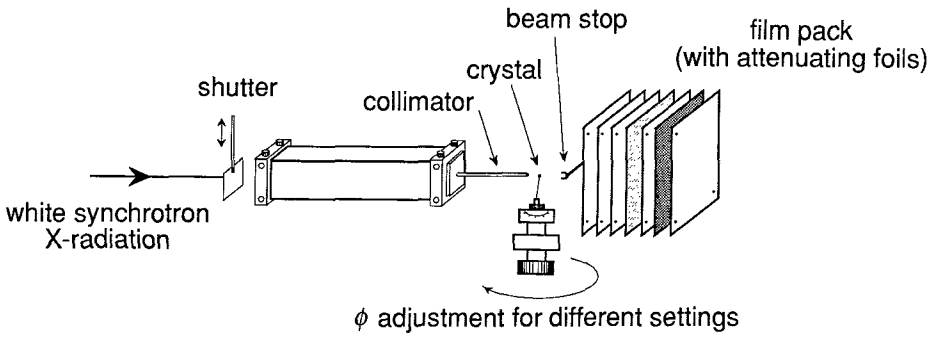

Figure 29. Experimental configuration for single-crystal Laue diffraction work on typical inorganic or small molecule systems.

number of crystal orientation settings (the number required depending on crystal symmetry) (figure 29). Placing all of the measured intensities on the same absolute scale requires that the incident intensity distribution, and all relevant wavelength dependent intensity corrections, be known with reasonable precision. The ideal scenario has a limited pre-selected range of wavelengths impinging on the sample, so that the problems associated with simultaneous recording of a large percentage of higher harmonics (which complicate data analysis), and with radiation damage of the sample can be minimized.

The Laue method has been applied to measurements of crystallite mosaicity (Andrews *et al.* 1987) and dimensions (Kalman *et al.* 1979). The potential for structure refinements using Laue diffraction patterns accumulated with SR radiation was demonstrated in 1983 (Wood *et al.* 1983). Residuals typically obtained in such refinements remain rather modest, although, it should be noted, they are little worse than those common for data accumulated in monochromatic single counter mode. A direct comparison with a crystal structure refinement based on in-house data has been made (Gomez de Anderez *et al.* 1989) and structure solutions (Clucas *et al.* 1988, Harding *et al.* 1988) based on reflection intensities measured in Laue geometry have been demonstrated.

The required exposure time is extremely short, enabling sufficient data for structure determination to be accumulated in a few minutes (circumventing several of the problems encountered with monochromatic radiation in single counter mode). Single Laue exposures from macromolecular structures (Moffat *et al.* 1984, 1986) have been recorded in a few seconds at SRS, Daresbury (Hajdu *et al.* 1987, Reynolds *et al.* 1988) and, recently, measurements at CHESS on the enzyme lysozyme have demonstrated than an interpretable Laue diffraction pattern can be obtained in only eight bunches from the storage ring (figure 3), enabling diffraction patterns (and hence structural insight) to be accumulated on a micro-nanosecond time scale (Moffat *et al.* 1988). As experience is further gained, the precision and applicability of these techniques will certainly be extended. The potential interest in experiments that are time-resolved on these time scales on inorganic and heterogeneous catalyst systems is substantial.

8. Studies under non-ambient and time-resolved conditions

Opportunities for exploiting the characteristics of the synchrotron X-ray source for measurements under non-ambient or extreme conditions have already been cited several times during the preceding discussion. High-pressure structural research was

one of the first disciplines to develop diffraction methods suitable for exploiting these opportunities. An already considerable literature documents studies of phase diagrams and structural characteristics of a large number of materials under applied pressure (Ruoff 1988, Skelton *et al.* 1984), such as UC (Olsen *et al.* 1986), UP (Olsen *et al.* 1988), KNO_3 (Adams *et al.* 1988) and metal dichalcogenide lubricants (Skelton *et al.* 1987), studies under combined high pressure and high (Bassett 1985, Iwasaki *et al.* 1986, Manghnani *et al.* 1981) or low temperatures (Skelton *et al.* 1984). Measurements have also been described on materials subjected to external electric fields (Kvick 1988), or to combined low temperatures and magnetic fields (Nakajima 1987).

Time-resolved experiments can, as above, use the time structure that is intrinsic to the synchrotron source (figure 3) or, as has been typically the case to date, the brightness of the source that permits definitive data to be collected in shorter time-frames than is possible with conventional equipment. A variety of time-resolved studies have already been described (Bartunik 1984, Kosten and Arnold 1984), such as of doping reactions (Riekel 1985), phase transformations in polymers (Riekel 1988), crystallizations (for example of wax (Doyle *et al.* (1988)) and $AlPO_4$ (Neissendorfer *et al.* 1987a)), dissolutions (Pritzkow *et al.* 1988), and decompositions (for example of hydrargillite (Neissendorfer *et al.* 1987b), $CdCO_3$ (Schoonover and Lin 1988) and $Cd(OH)_2$ (Savborg *et al.* 1987)).

9. Conclusion

Diffraction experiments may exploit each of the special features of synchrotron radiation and have already been applied to a diverse range of topical structural problems. In studies of surface structures, grazing incidence X-ray diffraction (GIXD) experiments on surface reconstructions, overlayers of higher atomic number (Z) species and submerged interfaces have been described. A prototypical study of monolayers of oxygen adsorbed on a Cu(110) surface demonstrates that extensions to low-Z adsorbate systems (such as hydrocarbons) are feasible. Structural studies of a range of other boundaries or interfaces have also been reported. Experiments on small metal or metal oxide particles dispersed on supports have exploited anomalous scattering effects to enhance sensitivity to the dispersed phase. Anomalous scattering studies can also assist structure solutions, or potentially improve the definition to which target atomic structural parameters can be defined. A range of synchrotron X-ray diffraction techniques have been applied to determinations of bulk crystal structures. High-resolution powder diffraction has assisted phase identification, provided more reliable quantitative data on peak broadening effects (such as arise from finite particle sizes or stacking disorder), enabled studies of subtle superstructures and a growing number of *ab initio* structure solutions, and permitted Rietveld refinements of a range of inorganic materials. Single-crystal diffraction techniques for inorganic and small molecule work are currently less well developed, but the potential for performing measurements on individual crystallites in the micrometre size regime has been demonstrated, a small number of successful structure refinements have been described, and ongoing developments in detector technology will likely facilitate further applications. Single-crystal Laue diffraction methods have been also applied successfully to structure refinements and solutions. In the Laue configuration, data sufficient for structure definition can be recorded on a very short time scale (in the micro-nanosecond regime). Potentially, therefore, structural changes that occur over these time scales might be followed. A range of studies that are time-resolved (on

somewhat longer scales), and various studies under non-ambient conditions (such as at high or low temperatures, at extreme pressures, or under applied magnetic and electric fields) have already been described. These various areas of application ensure an exciting future for synchrotron X-ray diffraction studies of inorganic and heterogeneous catalyst systems.

Glossary of acronyms

DAXD	Differential anomalous X-ray diffraction
DAXS	Differential anomalous X-ray scattering
DDP	Differential diffraction pattern
EXAFS	Extended X-ray absorption fine structure
GIXD	Grazing incidence X-ray diffraction
GIXS	Grazing incidence X-ray scattering
LEED	Low-energy electron diffraction
NEXAFS	Near-edge X-ray absorption fine structure
NSLS	National Synchrotron Light Source (at Brookhaven National Laboratory, see table 3)
PXD	Powder X-ray diffraction
SEXAFS	Surface extended X-ray absorption fine structure
SR	Synchrotron radiation
SXD	Single-crystal X-ray diffraction

Acknowledgments

We acknowledge those at Exxon Research and Engineering Company who have contributed to the development and application of synchrotron X-ray diffraction techniques for catalyst systems. A large number of individuals have contributed both directly and indirectly to our work that is mentioned here, most notably P. M. Eisenberger, D. E. Moncton, R. C. Hewitt, K. L. D'Amico, H. E. King, M. G. Sansone, S. Bennett, R. Abramowitz, M. A. Modrick, G. Hughes, M. E. Leonowicz, G. B. Ansell, C.-Z. Yang, R. H. Jones, D. Xie, J. Marsh, M. M. J. Treacy, D. E. W. Vaughan, J. Marsch and B. Weisel.

References

ADAMS, D. M., HATTON, P. D., HEATH, A. E., and RUSSELL, D. R., 1988, *J. Phys.* C, **21**, 505.

AKIMOTO, K., MIZUKI, J., TATSUMI, T., AIZAKI, N., and MATSUI, J., 1987, *Surf. Sci.*, **183**, L297.

ALS-NIELSEN, J., 1987, *Top. Curr. Phys.*, **43**, 181.

ALS-NIELSEN, J., CHRISTENSEN, F., and PERSHAN, P. S., 1982, *Phys. Rev. Lett.*, **48**, 1107.

AMEMIYA, Y., SATO, Y., MATSUSHITA, T., CHIKAWA, J., WAKABAYASHI, K., and MIYAHARA, J., 1988, *Top. Curr. Chem.*, **147**, 121.

ANDREWS, S. J., HAILS, J. E., HARDING, M. M., and CRUICKSHANK, D. W. J., 1987, *Acta crystallogr.* A, **43**, 70.

ANDREWS, S. J., PAPIZ, M. Z., MCMEEKING, R., BLAKE, A. J., LOWE, B. M., FRANKLIN, K. R., HELLIWELL, J. R., and HARDING, M. M., 1988, *Acta crystallogr.* B, **44**, 73.

ATTFIELD, J. P., CHEETHAM, A. K., COX, D. E., and SLEIGHT, A. W., 1988, *J. appl. Crystallogr.*, **21**, 452.

ATTFIELD, J. P., SLEIGHT, A. W., and CHEETHAM, A. K., 1986, *Nature*, **322**, 620.

BACHMANN, R., KOHLER, H., SCHULZ, H., and WEBER, H.-P., 1985, *Acta crystallogr.* A, **41**, 35.

BACHMANN, R., KOHLER, H., SCHULZ, H., WEBER, H.-P., KUPCIK, V., WENDSCHUH-JOSTIES, M., WOLF, A., and WULF, R., 1983, *Angew. Chem. Int. Ed.*, **22**, 1011.

BAERLOCHER, CH., and BARRER, R. M., 1972, *Z. Kristallogr., Kristallgeom., Kristallphys., Kristallchem.*, **136**, 245.

BART, J. C. J., 1986, *Adv. Catalysis*, **34**, 203.

BART, J. C. J., and VLAIC, G., 1987, *Adv. Catalysis*, **35**, 1.

BARTUNIK, H. D., 1984, *Rev. Phys. Appl.*, **19**, 671.

BASSETT, W. A., 1985, *Nucl. Instrum. Meth.* B, **10–11,** 309.
BIRGENEAU, R. J., BROWN, G. S., HORN, P. M., MONCTON, D. E., and STEPHENS, P. W., 1981, *J. phys. Chem.*, **14,** L49.
BOHR, J., FEIDENHANS'L, R., NIELSEN, M., TONEY, M., JOHNSON, R. L., and ROBINSON, I. K., 1985, *Phys. Rev. Lett.*, **54,** 1275.
BORDAS, J., GLAZER, A. M., HOWARD, C. J., and BOURDILLON, A. J., 1977, *Phil. Mag.*, **35,** 311.
BOUDART, M., DALLA BETTA, R. A., FOGER, K., LOFFLER, D. G., and SAMANT, M. G., 1985, *Science*, **228,** 717.
BOUDART, M., SANCHEZ, A. J., and DALLA BETTA, B. R., 1983, *J. Am. chem. Soc.*, **105,** 6501.
BRECK, D. W., and FLANIGEN, E. M., 1968, *Molecular Sieves*, edited by R. M. Barrer (London: Society for Chemical Industry), pp. 47–61.
BURAS, B., 1980, *Accuracy in Powder Diffraction*, NBS Special Publication No. 567 (Washington: National Bureau of Standards), pp. 33–54.
BURAS, B., GERWARD, L., GLAZER, A. M., HIDAKA, M., and OLSEN, J. S., 1979, *J. appl. Cryst.*, **12,** 531.
CLAUSEN, B. S., LENGELER, B., and TOPSOE, H., 1986, *Polyhedron*, **5,** 199.
CLAUSEN, B. S., NIEMANN, W., and TOPSOE, H., 1989, *Physica B, Amsterdam*, **158,** 160.
CLUCAS, J. A., HARDING, M. M., and MAGINN, S. J., 1988, *J. chem. Soc. chem. Commun*, 185.
CORCORAN, E. W., NEWSAM, J. M., KING, H. E., and VAUGHAN, D. E. W., 1989, *Zeolite Synthesis* (ACS Symposium Series 398), edited by M. Occelli and H. E. Robson (Washington: American Chemical Society), pp. 603.
COX, D. E., HASTINGS, J. B., CARDOSO, L. P., and FINGER, L. W., 1986, *High Resolution Powder Diffraction*, Materials Science Forum Vol. 9, edited by C. R. A. Catlow (Aedermannsdorf: Trans. Tech.), pp. 1–20.
COX, D. E., HASTINGS, J. B., THOMLINSON, W., and PREWITT, C. T., 1983, *Nucl. Instrum. Meth.*, **208,** 573.
DE ANGELIS, R. J., DHERE, A. G., MAGINNIS, M. A., REUCROFT, P. J., ICE, G. E., and HABENSCHUSS, A., 1987, *Adv. X-Ray Anal.*, **30,** 389.
DEEM, M. W., and NEWSAM, J. M., 1989, *Nature*, **342,** 260.
DELPRATO, F., GUTH, J. L., HUVE, L., BARON, J., DELMOTTE, L., SOULARD, M., ANGLEROT, D., and ZIVKOV, C., 1989, *Zeolites for the Nineties* (Recent research reports of the Eighth International Zeolite Conference, Amsterdam), pp. 127–128.
DENLEY, D. R., RAYMOND, R. H., and TANG, S. C., 1984, *J. Catalysis*, **87,** 414.
DOCHERTY, R., EL-KORASHY, A., JENNISSEN, H. D., KLAPPER, H., ROBERTS, K. J., and SCHEFFEN, L. T., 1988, *J. appl. Crystallogr.*, **21,** 406.
DOSCH, H., BATTERMAN, B. W., and WACK, D. C., 1986, *Phys. Rev. Lett.*, **56,** 1144.
DOYLE, S., ROBERTS, K. J., SHERWOOD, J. N., CLARK, S. M., and HAUSERMAN, D., 1988, *J. Cryst. Growth*, **88,** 306.
DRING, I. S., OLDMAN, R. J., STOCKS, A., WALBRIDGE, D. J., FALLA, N., ROBERTS, K. J., and PIZZINI, S., 1989, *Synchrotron Radiation in Materials Science*, MRS Symposium Proceedings Vol. 143, edited by R. Clark, J. L. Gland and J. H. Weaver (Pittsburgh: Materials Research Society), pp. 169–174.
EISENBERGER, P., and MARRA, W. C., 1981, *Phys. Rev. Lett.*, **46,** 1081.
EISENBERGER, P., NEWSAM, J. M., LEONOWICZ, M. E., and VAUGHAN, D. E. W., 1984, *Nature*, **309,** 45.
ERNST, S., KOKOTAILO, G. T., and WEITKAMP, J., 1987, *Zeolites*, **7,** 180.
FANKUCHEN, I., 1937, *Nature*, **139,** 193.
FEIDENHANS'L, R., 1990, *Surf. Sci. Reports*, **10,** 105.
FISHER, G. R., and BARNES, P., 1984, *J. appl. Crystallogr.*, **17,** 231.
FUOSS, P. H., LIANG, K. S., and EISENBERGER, P., 1990, *Synchrotron Radiation Research: Advances in Surface Science*, edited by R. Z. Bachrach (New York: Plenum) (to be published).
FYFE, C. A., GIES, H., KOKOTAILO, G. T., MARLER, B., and COX, D. E., 1990, *J. phys. Chem.* (to be published).
FYFE, C. A., GIES, H., KOKOTAILO, G. T., PASZTOR, C., STROBL, H., and COX, D. E., 1989, *J. Am. chem. Soc.*, **111,** 2470.
GIBBS, D., HARSHMAN, D. R., ISAACS, E. D., MCWHAN, D. B., MILLS, D., and VETTIER, C., 1988, *Phys. Rev. Lett.*, **61,** 1241.

GMÜR, N. F., THOMLINSON, W., and WHITE-DE PACE, S. M., 1989, *NSLS User's Manual: Guide to the VUV and X-ray Beamlines (BNL 42276)* (Upton, New York: Brookhaven National Laboratory).

GOMEZ DE ANDEREZ, D., HELLIWELL, M., HABASH, J., DODSON, E. J., HELLIWELL, J. R., BAILEY, P. D., and GAMMON, R. E., 1989, *Acta crystallogr.* B, **45,** 482.

GRAEFF, W., 1985, *Z. Phys.* B, **61,** 469.

GREAVES, G. N., 1988, *Catal. Today*, **2,** 581.

GREENHOUGH, T. J., HELLIWELL, J. R., and RULE, S. A., 1983, *J. appl. Crystallogr.*, **16,** 242.

GRUZALSKI, G. R., 1984, *Surf. Sci.*, **147,** L623.

GUSS, J. M., MERRITT, E. A., PHIZACKERLY, R. P., HEDMAN, B., MURATA, M., HODGSON, K. O., and FREEMAN, H. C., 1988, *Science*, **241,** 806.

HAJDU, J., MACHIN, P. A., CAMPBELL, J. W., GREENHOUGH, T. J., CLIFTON, I. J., ZUREK, S., GLOVER, S., JOHNSON, L. N., and ELDER, M., 1987, *Nature*, **329,** 178.

HARADA, S., YASUI, M., MURAKAWA, K., KASAI, N., and SATOW, Y., 1986, *J. appl. Crystallogr.*, **19,** 448.

HARDING, M. M., 1988, *Chemical Crystallography using Pulsed Neutrons and Synchrotron X-Rays*, NATO ASI Series C Vol. 221, edited by M. A. Carrondo and G. A. Jeffrey (Dordrecht: Reidel), pp. 537–561.

HARDING, M. M., MAGINN, S. J., CAMPBELL, J. W., CLIFTON, I., and MACHIN, P., 1988, *Acta crystallogr.* B, **44,** 142.

HART, M., 1975, *J. appl. Crystallogr.*, **8,** 436.

HART, M., PARRISH, W., and MASCIOCCHI, N., 1987, *Appl. Phys. Lett.*, **50,** 897.

HASTINGS, J. B., THOMLINSON, W., and COX, D. E., 1984, *J. appl. Crystallogr.*, **17,** 85.

HEALD, S. M., 1988, *X-ray Absorption*, Chemical Analysis Vol. 92, edited by D. C. Koningsberger and R. Prins (New York: Wiley), pp. 87–118.

HELLIWELL, J. R., 1984, *Rep. Prog. Phys.*, **47,** 1403.

HENRION, J., and RHEAD, G. E., 1972, *Surf. Sci.*, **29,** 20.

HERRON, N., WANG, Y., EDDY, M. M., STUCKY, G. D., COX, D. E., MOLLER, K., and BEIN, T., 1989, *J. Am. chem. Soc.*, **111,** 530.

HEWITT, R. C., SANSONE, M. G., LIANG, K. S., MONCTON, D. E., and D'AMICO, K. L., 1989 (unpublished).

HIBBLE, S. J., CHEETHAM, A. K., BOGLE, A. R. L., WAKERLEY, H. R., and COX, D. E., 1988, *J. Am. chem. Soc.*, **110,** 3295.

HIBBLE, S. J., CHEETHAM, A. K., and COX, D. E., 1987, *Inorg. Chem.*, **26,** 2389.

HIGGINS, J. B., LAPIERRE, R. B., SCHLENKER, J. L., ROHRMAN, A. C., WOOD, J. D., KERR, G. T., and ROHRBAUGH, W. J., 1988, *Zeolites*, **8,** 446.

HOECHE, H. R., SCHULZ, H., WEBER, H. P., BELZNER, A., WOLF, A., and WULF, R., 1986, *Acta crystallogr.* A, **42,** 106.

HOESLER, W., and MORITZ, W., 1986, *Surf. Sci.*, **175,** 63.

HUANG, T. C., HART, M., PARRISH, W., and MASCIOCCHI, N., 1987a, *J. appl. Phys.*, **61,** 2813.

HUANG, T. C., TONEY, M. F., BRENNAN, S., and REK, Z., 1987b, *Thin Solids Films*, **154,** 439.

IWASAKI, H., KIKEGAWA, T., FUJIMURA, T., ENDO, S., AKAHAMA, Y., AKAI, T., SHIMOMURA, O., YAMAOKA, S., YAGI, T., *et al.*, 1986, *Physica* B+C, **140,** 301.

JOYNER, R. W., and MEEHAN, P., 1983, *Vacuum*, **33,** 691.

KALMAN, Z. H., STEINBERGER, I. T., and HASNAIN, S. S., 1979, *J. appl. Crystallogr.*, **12,** 525.

KARLE, J., 1989, *Phys. Today*, 22.

KING, H. E., and NEWSAM, J. M., 1989 (in preparation).

KIRFEL, A., 1988, *Z. Kristallogr.*, **185,** 655.

KJAER, K., ALS-NIELSEN, J., HELM, C. A., TIPPMAN, K. P., and MOEHWALD, H., 1989, *J. phys. Chem.*, **93,** 3200.

KJAER, K., ALS-NIELSEN, J., HELM, C. A., LAXHUBER, L. A., and MOEHWALD, H., 1987, *Phys. Rev. Lett.*, **58,** 2224.

KJAER, K., NIELSEN, M., BOHR, J., LAUTER, H. J., and MCTAGUE, J. P., 1982, *Phys. Rev.* B, **26,** 5168.

KOCH, E.-E., 1983, *Handbook on Synchrotron Radiation*, Vol. 1 (Amsterdam: North-Holland).

KOCHUBEI, D. J., and ZAMARAEV, K. J., 1985, *Advances in Catalysis, (Proceedings of the Seventh National Symposium Catalysis)*, edited by T. S. R. Prasada Rao (New York: Wiley), pp. 287–294.

KÖHLER, J., SIMON, A., HIBBLE, S. J., and CHEETHAM, A. K., 1988, *J. less-common Metals*, **142,** 123.

KOKOTAILO, G. T., CHU, P., LAWTON, S. L., and MEIER, W. M., 1978, *Nature*, **275,** 119.

KONINGSBERGER, D. C., DUIVENVOORDEN, F. B. M., KIP, B. J., and SAYERS, D. E., 1986, *J. Phys., Paris*, **1**, C8–255.
KONINGSBERGER, D. C., and SAYERS, D. E., 1985, *Solid St. Ionics*, **16**, 23.
KORTRIGHT, J. B., and BIENENSTOCK, A., 1988, *Phys. Rev.* B, **37**, 2979.
KOSTEN, K., and ARNOLD, H., 1984, *J. appl. Crystallogr.*, **17**, 206.
KOZLOWSKI, R., PETTIFER, R. F., and THOMAS, J. M., 1983a, *J. chem. Soc. chem. Commun*, 438; 1983b, *J. phys. Chem.*, **87**, 5172; 1983c, *Ibid.*, **87**, 5176.
KUNZ, C., 1979, *Topics in Current Physics—Synchrotron Radiation; Techniques and Applications* (Heidelberg: Springer).
KUPCIK, V., 1988, *Z. Kristallogr.*, **185**, 673.
KURIYAMA, M., BOETTINGER, W. J., and COHEN, G. G., 1982, *Ann. Rev. Mater. Sci.*, **12**, 23.
KURIYAMA, M., STEINER, B., DOBBYN, R. C., LAOR, U., LARSON, D., and BROWN, M., 1988, *Phys. Rev.* B, **38**, 12421.
KVICK, Å., 1988, *Chemical Crystallography with Pulsed Neutrons and Synchrotron X-Rays*, Nato Advanced Study Institute Series C, Vol. 221, edited by M. A. Carrondo and G. A. Jeffrey (Dordrecht: Reidel), pp. 187–203.
KVICK, Å., and ROHRBAUGH, W. J., 1988 (unpublished).
LAPIERRE, R. B., ROHRMAN, A. C. J., SCHLENKER, J. L., WOOD, J. D., RUBIN, M. K., and ROHRBAUGH, W. J., 1985, *Zeolites*, **5**, 346.
LARSON, B. C., WHITE, C. W., NOGGLE, T. S., and MILLS, D., 1982, *Phys. Rev. Lett.*, **48**, 337.
LE BAIL, A., DUROY, H., and FOURQUET, J. L., 1988, *Mater. Res. Bull.*, **23**, 447.
LEE, P., GAO, Y., SHEU, H. S., PETRICEK, V., RESTORI, R., COPPENS, P., DAROVSKIKH, A., PHILLIPS, J. C., SLEIGHT, A. W., and SUBRAMANIAN, M. A., 1989, *Science*, **244**, 62.
LEE, P. A., CITRIN, P. H., EISENBERGER, P., and KINCAID, B. M., 1981, *Rev. mod. Phys.*, **53**, 769.
LEHMANN, M. S., CHRISTENSEN, A. N., FJELLVAG, H., FEIDENHANS'L, R., and NIELSEN, M., 1987, *J. appl. Crystallogr.*, **20**, 123.
LEHMANN, M. S., CHRISTENSEN, A. N., NIELSEN, M., FEIDENHANS'L, R., and COX, D. E., 1988, *J. appl. Crystallogr.*, **21**, 905.
LEONOWICZ, M. E., JOHNSON, J. W., BRODY, J. F., SHANNON, H. F., and NEWSAM, J. M., 1985, *J. solid-st. Chem.*, **56**, 370.
LIANG, K. S., CHIANELLI, R. R., CHIEN, F. Z., and MOSS, S. C., 1986, *J. non-crystalline Solids*, **79**, 251.
LIANG, K. S., FUOSS, P. H., HUGHES, G. J., and EISENBERGER, P., 1985, *The Structure of Surfaces*, edited by M. A. Van Hove and S. Y. Tong (Berlin: Springer), pp. 246.
LIANG, K. S., HUGHES, G. J., CHIEN, F. Z., SINFELT, J. H., MEITZNER, G. D., and LEE, C. H., 1989a (to be published).
LIANG, K. S., HUGHES, G. J., and SINFELT, J. H., 1987, *J. chem. Phys.*, **86**, 2352; 1989b, *Physica* B, **158**, 135.
LIANG, K. S., HUGHES, G. J., SIROTA, E. B., NEWSAM, J. M., and D'AMICO, K. L., 1989c (in preparation).
LIANG, K. S., SIROTA, E. B., D'AMICO, K. L., HUGHES, G. J., and SINHA, S. K., 1988, *Phys. Rev. Lett.*, **59**, 2447.
LIGHTFOOT, P., CHEETHAM, A. K., and SLEIGHT, A. W., 1987, *Inorg. Chem.*, **26**, 3544.
LIM, G., PARRISH, W., ORTIZ, C., BELLOTTO, M., and HART, M., 1987, *J. Mater. Res.*, **2**, 471.
LIN, B., PENG, J. B., KETTERSON, J. B., and DUTTA, P., 1988, *Thin solid Films*, **159**, 111.
LOEWENSTEIN, W., 1954, *Am. Mineral.*, **39**, 92.
MANGHNANI, M. H., SKELTON, E. F., MING, L. C., JAMIESON, J. C., QADRI, S., SCHIFERL, D., and BALOGH, J., 1981, *Physics of Solids at High Pressure*, edited by J. S. Schilling and R. N. Shelton (Amsterdam: North-Holland), pp. 47–55.
MAO, H. K., JEPHCOAT, A. P., HEMLEY, R. J., FINGER, L. W., ZHA, C. S., HAZEN, R. M., and COX, D. E., 1988, *Science*, **239**, 1131.
MAREZIO, M., COX, D. E., ROSSEL, C., and MAPLE, M. B., 1988, *Solid St. Commun.*, **67**, 831.
MARR, G. V., 1987, *Handbook on Synchrotron Radiation*, Vol. 2 (Amsterdam: North-Holland).
MARRA, W. C., EISENBERGER, P., and CHO, A. Y., 1979, *J. appl. Phys.*, **50**, 6927.
MCCUSKER, L., 1988, *J. appl. Crystallogr.*, **21**, 305.
MCTAGUE, J. P., ALS-NIELSEN, J., BOHR, J., and NIELSEN, M., 1982, *Phys. Rev.* B, **25**, 7765.
MEIER, W. M., and OLSON, D. H., 1987, *Atlas of Zeolite Structure Types* (Guildford: Butterworths).

MEITZNER, G., VIA, G. H., LYTLE, F. W., FUNG, S. C., and SINFELT, J. H., 1988, *J. phys. Chem.*, **92,** 2925.
MEITZNER, G., VIA, G. H., LYTLE, F. W., and SINFELT, J. H., 1987, *J. chem. Phys.*, **87,** 6354.
MILCH, J. R., GRUNER, S. M., and REYNOLDS, G. T., 1982, *Nucl. Instrum. Meth.*, **201,** 43.
MILLS, D. M., 1984, *Phys. Today*, 22.
MIZUKI, J., AKIMOTO, K., HIROSAWA, I., HIROSE, K., MIZUTANI, T., and MATSUI, J., 1988, *J. vac. Sci. Technol.* B, **6,** 31.
MOFFAT, K., BILDERBACK, D., SCHILDKAMP, W., and VOLZ, K., 1986, *Nucl. Instrum. Meth.* A, **246,** 627.
MOFFAT, K., SCHILDKAMP, W., BILDERBACK, D., and SZEBENYI, M., 1988 (unpublished).
MOFFAT, K., SZEBENYI, D., and BILDERBACK, D., 1984, *Science, Washington, D.C.*, **223,** 1423.
MOLLER, K., EDDY, M. M., STUCKY, G. D., HERRON, N., and BEIN, T., 1989a, *J. Am. chem. Soc.*, **111,** 2564.
MOLLER, K., KONINGSBERGER, D. K., and BEIN, T., 1989b, *J. phys. Chem.*, **93,** 6116.
MONCTON, D., and BROWN, G., 1990, *Handbook on Synchrotron Radiation*, Vol. 3 (Amsterdam: North-Holland).
MONCTON, D. E., D'AMICO, K. L., BOHR, J., ALS-NIELSEN, J., FLEMING, R. M., REMEIKA, J. P., and VAKNIN, D., 1987 (unpublished).
MOORE, P. B., and SMITH, J. V., 1964, *Mineralog. Mag.*, **35,** 1008.
MORAWECK, B., CLUGNET, G., and RENOUPREZ, A., 1986, *J. chim. Phys. phys. Chim. Biol.*, **83,** 265.
MORONEY, L. M., THOMPSON, P., and COX, D. E., 1988, *J. appl. Crystallogr.*, **21,** 206.
NAKAJIMA, T., 1987, *Nucl. Instrum. Meth.* A, **261,** 308.
NEISSENDORFER, F., STEINIKE, U., TOLOCHKO, B. P., and SHEROMOV, M. A., 1987a, *Nucl. Instrum.* A, **261,** 216; 1987b, *Ibid.*, **261,** 219.
NEWSAM, J. M., 1986, *Science*, **231,** 1093.
NEWSAM, J. M., and KING, H. E., 1987, *Acta crystallogr.* A, **43,** Suppl., C–259.
NEWSAM, J. M., KING, H. E., and LIANG, K. S., 1989a, *Advances in X-ray Analysis*, edited by C. S. Barrett, J. V. Gilfrich, R. Jenkins, T. C. Huang and P. K. Predecki (New York: Plenum), pp. 9–20.
NEWSAM, J. M., TREACY, M. M. J., KOETSIER, W. T., and DEGRUYTER, C. B., 1988, *Proc. R. Soc., London*, A, **420,** 375.
NEWSAM, J. M., TREACY, M. M. J., VAUGHAN, D. E. W., STROHMAIER, K. G., and MORTIER, W. J., 1989b, *J. chem. Soc. chem. Commun.*, 493.
NEWSAM, J. M., TREACY, M. M. J., YANG, C.-Z., VAUGHAN, D. E. W., VERDUIJN, J. P., and SCHWEIZER, A. E., 1989c (unpublished).
NEWSAM, J. M., and VAUGHAN, D. E. W., 1985, *Zeolites: Synthesis, Structure, Technology and Application*, Studies in Surface Science and Catalysis No. 24, edited by B. Drzaj, S. Hocevar and S. Pejovnik (Amsterdam: Elsevier), pp. 239–248.
NEWSAM, J. M., YANG, C.-Z., TREACY, M. M. J., VAUGHAN, D. E. W., and STROHMAIER, K. G., 1989a (in preparation).
NEWSAM, J. M., YANG, C.-Z., VAUGHAN, D. E. W., STROHMAIER, K. G., RICE, S. B., and TREACY, M. M. J., 1989b (in preparation).
NIELSEN, F. S., LEE, P., and COPPENS, P., 1986, *Acta crystallogr.* B, **42,** 359.
NIELSEN, M., ALS-NIELSEN, J., BOHR, J., MCTAGUE, J. P., MONCTON, D. E., and STEPHENS, P. W., 1987, *Phys. Rev.* B, **35,** 1419.
NOMURA, M., 1988, *Shokubai*, **30,** 15.
NØRLUND CHRISTENSEN, A., COX, D. E., and LEHMANN, M. S., 1989, *Acta chem. Scand.*, **43,** 19.
OHSUMI, K., TSUTSUI, K., TAKEUCHI, Y., and TOKONAMI, M., 1987, *Acta crystallogr.* A, **43,** Suppl., C–255.
OLSEN, J. S., GERWARD, L., BENEDICT, U., DABOS, S., and VOGT, O., 1988, *Phys. Rev.* B, **37,** 8713.
OLSEN, J. S., GERWARD, L., BENEDICT, U., ITIE, J. P., and RICHTER, K., 1986, *J. less-common metals*, **121,** 445.
PARRISH, W., and HART, M., 1987, *Z. Kristallogr.*, **179,** 161.
PARRISH, W., HART, M., and HUANG, T. C., 1986, *J. appl. crystallogr.*, **19,** 92.
PAWLEY, G. S., 1981, *J. appl. Crystallogr.*, **14,** 357.
PHILLIPS, J. C., and HODGSON, K. O., 1980, *Synchrotron Radiation Research*, edited by H. Winick and S. Doniach (New York: Plenum), pp. 565–605.

PHILLIPS, J. C., WLODAWER, A., YEVITZ, M. M., and HODGSON, K. O., 1976, *Proc. Natl Acad. Sci. U.S.A.*, **73,** 128.

PRIESKE, W., RIEKEL, C., KOCH, M. H. J., and ZACHMANN, H. G., 1983, *Nucl. Instrum. Meth.*, **208,** 435.

PRITZKOW, W., RENTSCH, H., GROSSHANS, W. A., and WROBLEWSKI, T., 1988, *Cryst. Res. Technol.*, **23,** 1289.

RAMASESHAN, S., and ABRAHAMS, S. C., 1975, *Anomalous Scattering* (Copenhagen: Munksgaard).

REYNOLDS, C. D., STOWELL, B., JOSHI, K. K., HARDING, M. M., MAGINN, S. J., and DODSON, G. G., 1988, *Acta crystallogr.* B, **44,** 512.

RICE, S. B., 1989, *Origin and Structural State of the Zeolite Ferrierite in Rhyolitic Tuffs, Lovelock, Nevada: An Electron-optical Study* (Lehigh University).

RIECK, W., EULER, H., SCHULZ, H., and SCHILDKAMP, W., 1988, *Acta crystallogr.* A, **44,** 1099.

RIEKEL, C., 1985, *Electronic Properties of Polymers and Related Compounds*, Springer Series in Solid State Science, Vol. 63 (Heidelberg: Springer), pp. 35–40.

RIEKEL, C., 1988, *Chemical Crystallography with Pulsed Neutrons and Synchrotron X-Rays*, Nato Advanced Study Institute Series C, Vol. 221, edited by M. A. Carrondo and G. A. Jeffrey (Dordrecht: Reidel), pp. 443–484.

ROBERTS, K. J., SHERWOOD, J. N., BOWEN, D. K., and DAVIES, S. T., 1983, *Mater. Lett.*, **2,** 104.

ROBINSON, I. K., 1990, *Handbook on Synchrotron Radiation*, Vol. 3, edited by D. Moncton and G. Brown (Amsterdam: North-Holland) (to be published).

ROBINSON, I. K., TUNG, R. T., and FEIDENHANS'L, R., 1988, *Phys. Rev.* B, **38,** 3632.

ROBINSON, I. K., WASKIEWICZ, W. K., FUOSS, P. H., STARK, J. B., and BENNET, P. A., 1986, *Phys. Rev.* B, **33,** 7013.

ROSENBAUM, G., HOLMES, K. C., and WITZ, J., 1971, *Nature*, **230,** 434.

RUDOLF, P. R., SALDARRIAGA-MOLINA, C., and CLEARFIELD, A., 1986, *Inorg. Chem.*, **90,** 6122.

RUOFF, A. L., 1988, *Accts Chem. Res.*, **21,** 223.

SAKAMAKI, T., HOSOYA, S., TAGAI, T., OHSUMI, K., and SATOW, Y., 1984, *J. appl. Crystallogr.*, **17,** 219.

SAMANT, M. G., BERGERET, G., MEITZNER, G., and BOUDART, M., 1988a, *J. phys. Chem.*, **92,** 3542.

SAMANT, M. G., BERGERET, G., MEITZNER, G., GALLEZOT, P., and BOUDART, M., 1988b, *J. phys. Chem.*, **92,** 3547.

SANKAR, G., VASUDEVAN, S., and RAO, C. N. R., 1986, *J. chem. Phys.*, **85,** 2291.

SAVBORG, O., SCHOONOVER, J. R., LIN, S. H., and EYRING, L., 1987, *J. solid-st. Chem.*, **68,** 214.

SCHOONOVER, J. R., and LIN, S. H., 1988, *J. solid-st. Chem.*, **76,** 143.

SEUL, M., EISENBERGER, P., and MCCONNELL, H. M., 1983, *Proc. Natl Acad. Sci. U.S.A.*, **80,** 5795.

SINFELT, J. H., 1983, *Bimetallic catalysts: Discoveries, concepts and applications* (New York: Wiley).

SINFELT, J. H., VIA, G. H., and LYTLE, F. W., 1978, *J. chem. Phys.*, **68,** 209; 1984, *Catal. Rev. Sci. Engng*, **26,** 81.

SKELTON, E. F., 1984, *Phys. Today*, **37,** 44.

SKELTON, E. F., WEBB, A. W., ELAM, W. T., WOLF, S. A., QADRI, S. B., HUANG, C. Y., CHAIKIN, P. M., LACOE, R. C., and GSCHNEIDNER, K. A., 1984, *High Pressure Sci. Technol.*, Pt 3, MRS Symposium Proceedings Vol. 22 (Pittsburgh, Pennsylvania: Materials Research Society), pp. 5–9.

SKELTON, E. F., WEBB, A. W., SCHAEFER, M. W., SCHIFERL, D., KATZ, A. I., HOCHHEIMER, H. D., and QADRI, S. B., 1987, *Adv. X-Ray Anal.*, **30,** 465.

SMITH, G. S., JOHNSON, Q. C., COX, D. E., SNYDER, R. L., SMITH, D. K., and ZALKIN, A., 1987, *Adv. X-Ray Anal.*, **30,** 383.

SOKOLOV, A. A., and TERNOV, I. M., 1968, *Synchrotron Radiation* (Oxford: Pergamon).

STOHR, J., 1985, *Z. Phys.* B, **61,** 439.

STOHR, J., 1988, *X-ray Absorption. Principles, Applications, Techniques of EXAFS, NEXAFS and XANES*, edited by D. C. Koningsberger and R. Prins (New York: Wiley), pp. 443–572.

STOHR, J., GLAND, J. L., KOLLIN, E. B., KOESTNER, R. J., JOHNSON, A. L., MUETTERTIES, E. L., and SETTE, F., 1984, *Phys. Rev. Lett.*, **53,** 2161.

STOHR, J., KOLLIN, E. B., FISCHER, D. A., HASTINGS, J. B., ZAERA, F., and SETTE, F., 1985, *Phys. Rev. Lett.*, **55,** 1468.

STUHRMANN, H. B., 1988, *Chemical Crystallography with Pulsed Neutrons and Synchrotron X-Rays*, Nato Advanced Study Institute Series C, Vol. 221, edited by M. A. Carrondo and G. A. Jeffrey (Dordrecht: Reidel), pp. 357–377.

TEMPLETON, D. H., and TEMPLETON, L. K., 1985, *Acta Crystallogr.* A, **41,** 365; 1989, *Synchrotron X-ray Scattering Studies of Catalysts,* MRS Symposium Proceedings Vol. 143, edited by J. L. Gland and S. Clark (Pittsburgh, Pennsylvania: Materials Research Society), pp. 177–184.

TEO, B. K., 1986, *EXAFS: Basic Principles and Data Analysis* (Berlin: Springer).

THOMPSON, P., COX, D. E., and HASTINGS, J. B., 1987, *J. appl. Crystallogr.*, **20,** 79.

THOMPSON, P., GLAZER, A. M., ALBINATI, A., and WORGAN, J. S., 1981, *J. appl. Crystallogr.*, **14,** 315.

TOBY, B. H., EDDY, M. M., FYFE, C. A., KOKOTAILO, G. T., STROBL, H., and COX, D. E., 1988, *J. Mater. Res.*, **3,** 563.

TREACY, M. M. J., and NEWSAM, J. M., 1988, *Nature*, **332,** 249.

TREACY, M. M. J., NEWSAM, J. M., BEYERLEIN, R. A., LEONOWICZ, M. E., and VAUGHAN, D. E. W., 1986, *J. chem. Soc. chem. Commun.*, 1211.

TREACY, M. M. J., NEWSAM, J. M., and DEEM, M. W., 1989, *Disorder in Crystalline Materials,* MRS Symposium Proceedings (Pittsburgh, Pennsylvania: Materials Research Society), pp. 497–502; 1990 (in preparation).

TREACY, M. M. J., NEWSAM, J. M., VAUGHAN, D. E. W., BEYERLEIN, R. A., RICE, S. B., and DE GRUYTER, C. B., 1988, *Microstructure and Properties of Catalysts,* MRS Symposium Proceedings, Vol. 111, edited by M. M. J. Treacy, J. M. White and J. M. Thomas (Pittsburgh, Pennsylvania: Materials Research Society), pp. 177–190.

TUOMI, T., NAUKKARINEN, K., and RABE, P., 1974, *Phys. Stat. sol.* A, **25,** 93.

TZOU, M. S., TEO, B. K., and SACHTLER, W. H. M., 1986, *Langmuir*, **2,** 773.

VAN HOVE, M. A., and TONG, S. Y., 1979, *Surface Crystallography by LEED* (Berlin: Springer); 1985, *The Structure of Surfaces* (Berlin: Springer).

VAUGHAN, D. E. W., 1989, *European Patent Application*, 0315, 461.

VAUGHAN, D. E. W., TREACY, M. M. J., NEWSAM, J. M., STROHMAIER, K. G., and MORTIER, W. J., 1989, *Zeolite Synthesis,* ACS Symposium Series 398, edited by M. Occelli and H. E. Robson (Washington: American Chemical Society), pp. 544–559.

VIA, G. H., MEITZNER, G., LYTLE, F. W., and SINFELT, J. H., 1983, *J. chem. Phys.*, **79,** 1527.

WARREN, B. E., 1969, *X-ray Diffraction* (New York: Addison-Wesley).

WILL, G., MASCIOCCHI, N., HART, M., and PARRISH, W., 1987a, *Acta crystallogr.* A, **43,** 677.

WILL, G., MASCIOCCHI, N., PARRISH, W., and HART, M., 1987b, *J. appl. Crystallogr.*, **20,** 394; 1988, *Ibid.*, **21,** 182.

WINICK, H., 1987, *Scient. Am.*, **257,** 88.

WINICK, H., and DONIACH, S., 1980, *Synchrotron Radiation Research* (New York: Plenum).

WOLF, S. G., LEISEROWITZ, L., LAHAV, M., DEUTSCH, M., KJAER, K., and ALS-NIELSEN, J., 1987, *Nature*, **328,** 63.

WOOD, I. G., THOMPSON, P., and MATTHEWMAN, J. C., 1983, *Acta crystallogr.* B, **39,** 543.

WÜSTEFELD, C., VOGT, T., LOECHNER, U., STRAEHLE, J., and FUESS, H., 1988, *Angew. Chem.*, **100,** 1013.

YOKOYAMA, T., KOSUGI, N., ASAKURA, K., IWASAWA, Y., and KURODA, H., 1986, *J. Phys., Paris*, **1,** C8–301.